ESRF

Pahtways for X-ray Nanometer Focusing

What are the Scientific Opportunities

Anatoly SNIGIREV

CHESS WS , 23-24 June, 2006

ERL :

Beam energy	$E = 5.3$ GeV	

<u>“high coherence” mode</u>

current	$I = 10$ mA	
betafunction	$\beta = 1$ m	(2.5 m; 12.5 m)
emittance	$\varepsilon = 0.015$ nm rad	

Source size:	(FWHM)	
$\sigma = 4\ \mu m$	$S = 10\ \mu m$	(esrf 25 x 900 μm^2)
Beam divergence	(FWHM)	
$\sigma' = 4\ \mu rad$	$S' = 10\ \mu rad$	(esrf 20 x 30 μrad^2)

Av. brilliance: 3 x 10^{22} ph / (s 0.1% mm^2 mrad^2)

Undulator X-ray beam (ESRF/ERL)

ESRF 200 mA

10^{13} ph/s/mm^2/Si-111

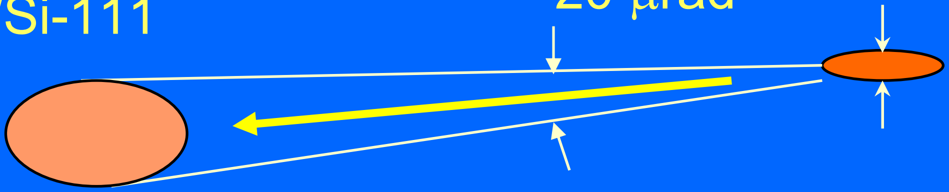

~ 20 μrad

high-β undulator

S_v = 25 μm
S_v = 900 μm

~1x1.5 mm^2 at 50 m

ERL 10 mA

section: β= 1 m

10^{14} ph/s/mm^2/Si-111

~ 10 μrad

S = 10 μm dia

∅ ~0.5 mm at 50 m

Why do we need a coherent beam for Microoptics?

Transverse coherence ~ Aperture of the optics
- Diffraction limited focusing at nm level
- Coherent secondary source - coherence inhancement

Aperture (acceptance) of nanooptics is about 50 -500 μm
resolution ~ 10 – 100 nm

for ERL : beamsize 500 μm dia at 50 m

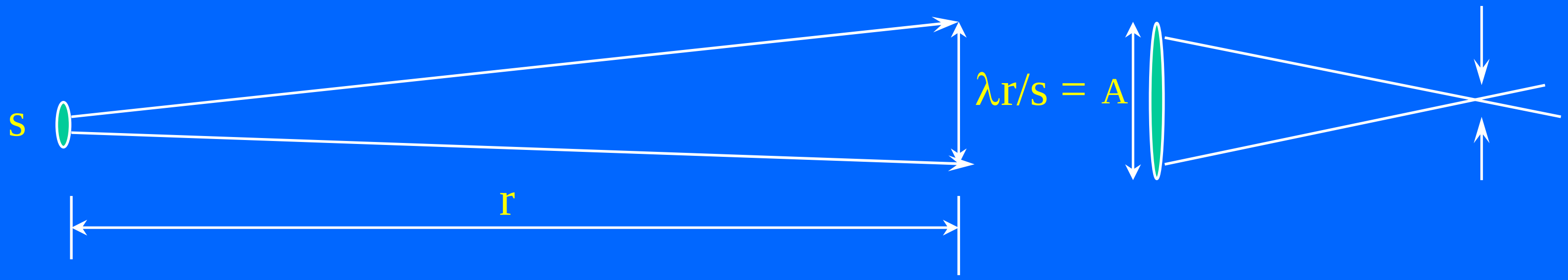

Focusing Optics for Hard X-rays: 6 - 60 (200) keV

	reflective				*diffractive*	*refractive*
	Kirkpatrick Baez systems		Capillaries	Waveguides	Fresnel Zone plates	Refractive lenses
	mirrors Kirkpatrick Baez, 1948	multilayers Underwood Barbee, 1986	Kreger 1948	Feng et al 1993	Baez 1952	Snigirev et al, 1996
	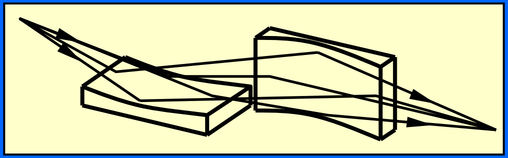		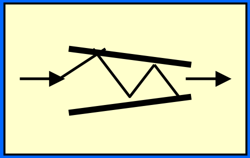	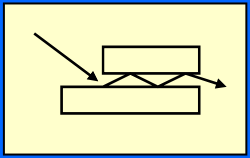	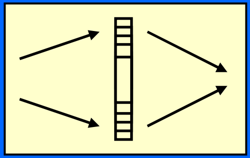	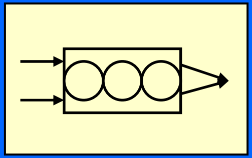
Energy	< 30 keV	< 80keV	< 20keV	< 20keV	< 30 keV (80)	<1 MeV
Bandwidth DE/E	w. b.	10^{-2}	w.b.	10^{-3}	10^{-3}	10^{-3}
resolution	**25 nm** Spring 8 2006	**40 nm** Hignette 2005	**50 nm** Bilderback 1994	**40x25 nm^2** Salditt 2004	**20 nm @ 20keV** APS, 2006 ~15nm<1keV	**50 nm** Schroer 2004

Fresnel Zone Plate (FZP)

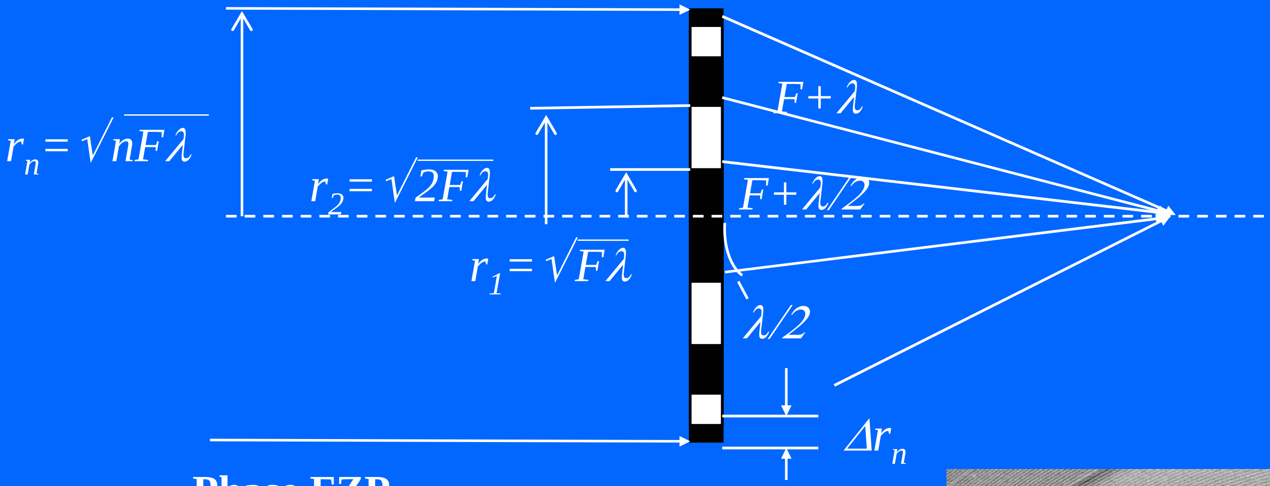

FZP parameters

A = 100 - 1000 µm
Δr_n = 0.05 - 0.3 µm
t_{Si} = 1 - 10 µm
F = 60 cm at at 4 - 12 keV
flux 10^{10} photons/sec

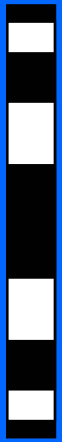

Amplitude FZP
alternate zones - opaque
efficiency ~ 10%

Phase FZP
alternate zones -
phase shifting
efficiency ~ 40%

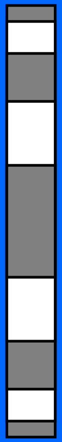

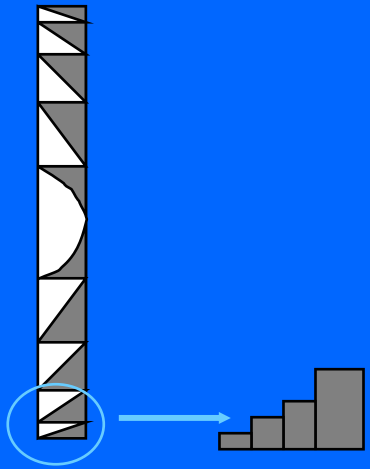

Kinoform FZP
(sawtooth profile)
efficiency ~ 70 - 100%

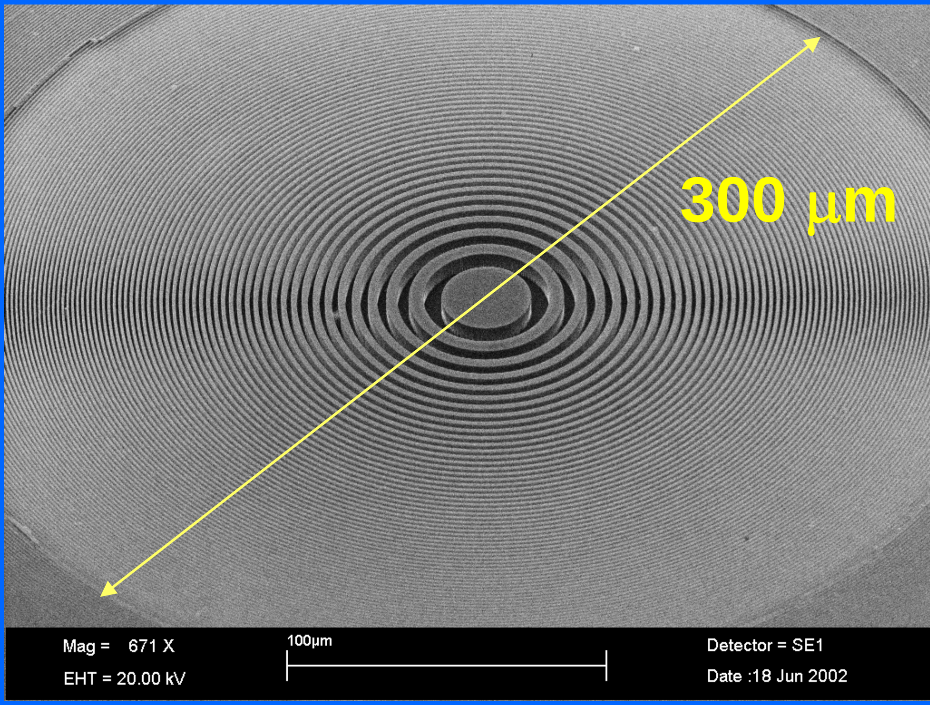

Res. ~ from 500 nm to 50 nm

FZP Si chip

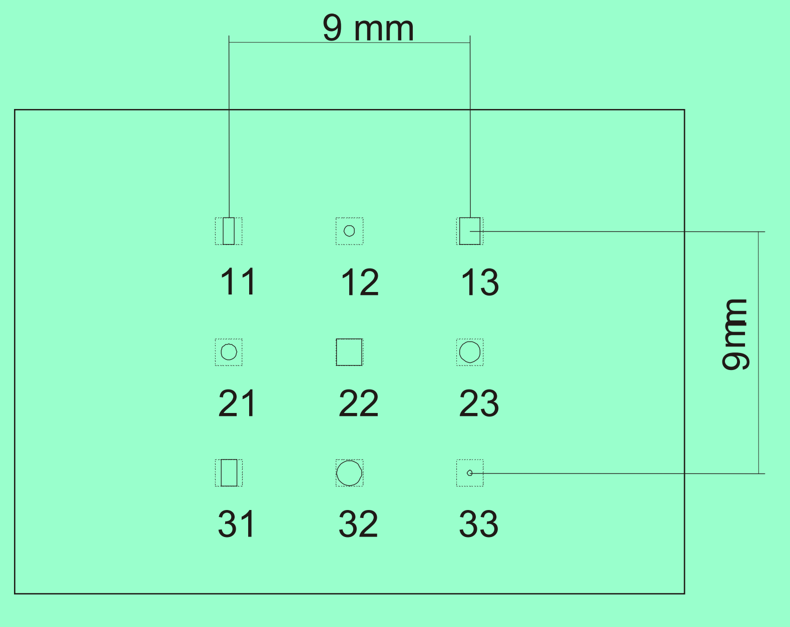

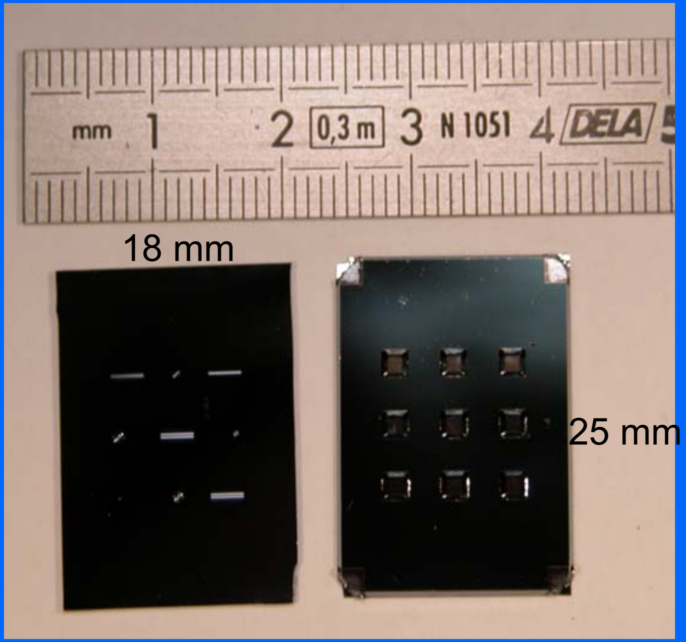

Lens parameters

$$A=2r_n = F\lambda / dr_n$$

DOE type	Focal length, F (cm) at 8 keV	Aperture of DOE, A (μm)	Outermost zone width, dr_n (μm)	Number of zones
33 (circular)	50	A=194	0.4	122
11 (linear)	100	A=387; L=1000	0.4	242
12 (circular)	100	A=387	0.4	242
21 (circular)	150	A=582	0.4	364
31 (linear)	150	A=582; L=1000	0.4	364
13 (linear)	200	A=775; L=1000	0.4	484
23 (circular)	200	A=775	0.4	484
22 (linear)	240	A=930; L=1000	0.4	582
32 (circular)	240	A=930	0.4	582

SEM images

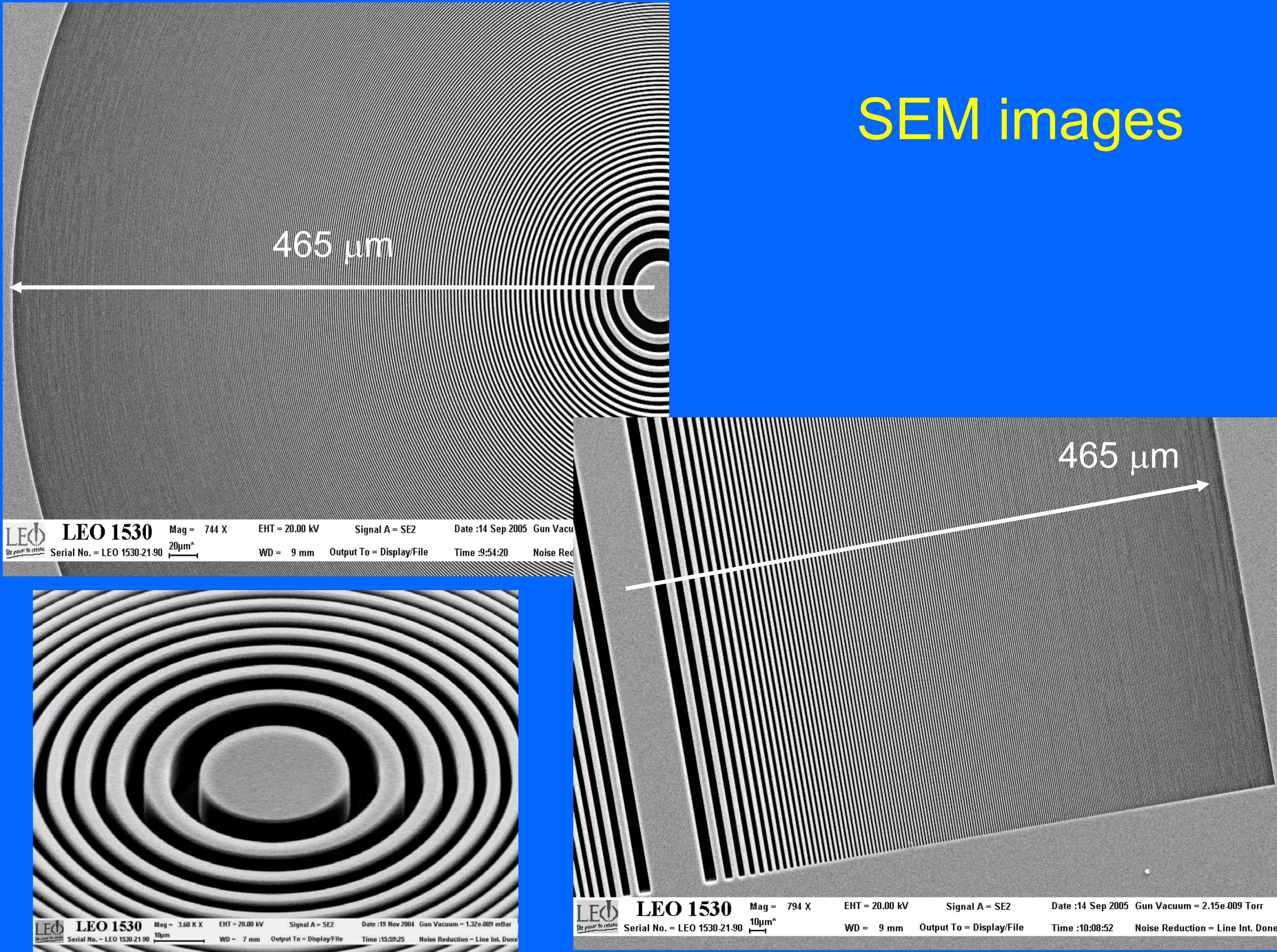
465 μm
LEO 1530
Mag = 744 X
EHT = 20.00 kV
Signal A = SE2
Date :14 Sep 2005
Gun Vacu
Serial No. = LEO 1530-21-90
20μm*
WD = 9 mm
Output To = Display/File
Time :9:54:20
Noise Red
465 μm
LEO 1530
Mag = 794 X
EHT = 20.00 kV
Signal A = SE2
Date :14 Sep 2005
Gun Vacuum = 2.15e-009 Torr
Serial No. = LEO 1530-21-90
10μm*
WD = 9 mm
Output To = Display/File
Time :10:08:52
Noise Reduction = Line Int. Done
LEO 1530
Mag = 3.68 K X
EHT = 20.00 kV
Signal A = SE2
Date :19 Nov 2004
Gun Vacuum = 1.32e-009 mBar
Serial No. = LEO 1530-21-90
10μm
WD = 7 mm
Output To = Display/File
Time :15:59:25
Noise Reduction = Line Int. Done

Stacking FZP

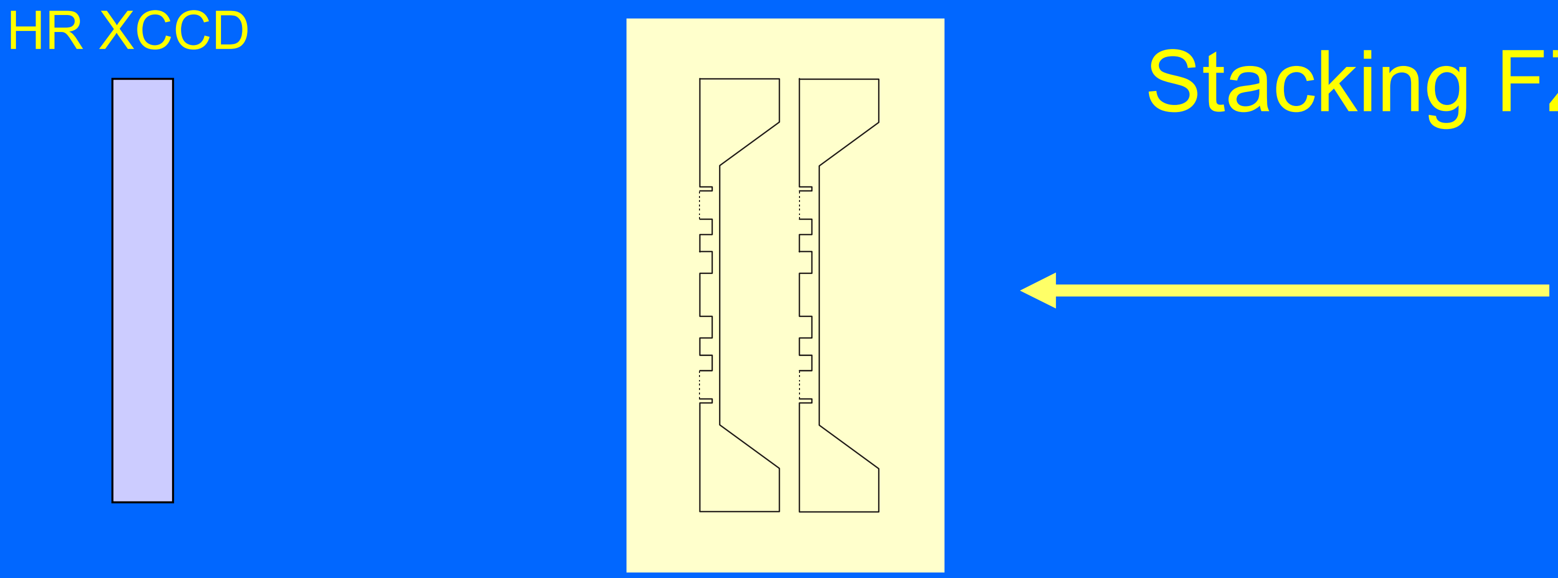

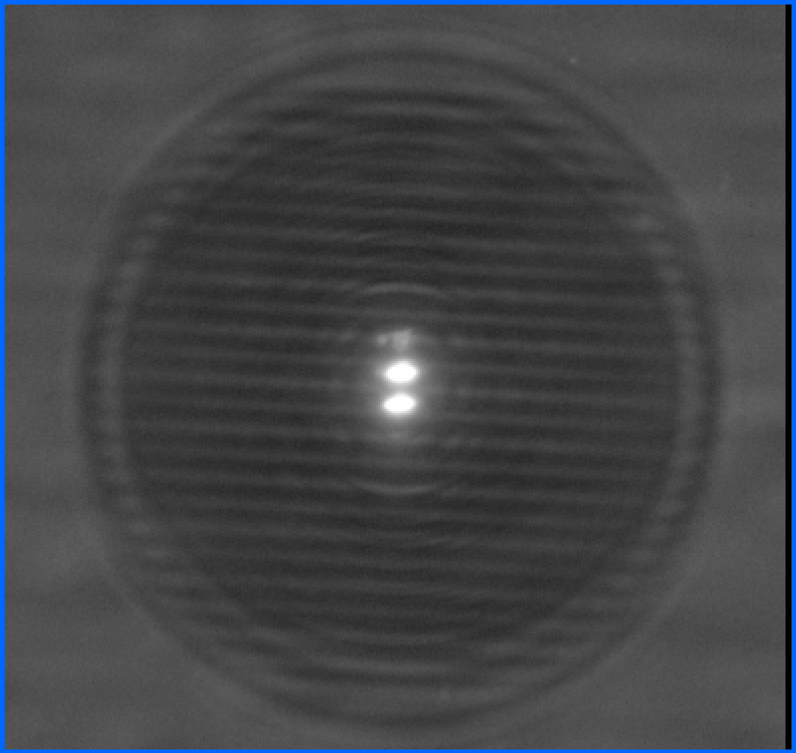

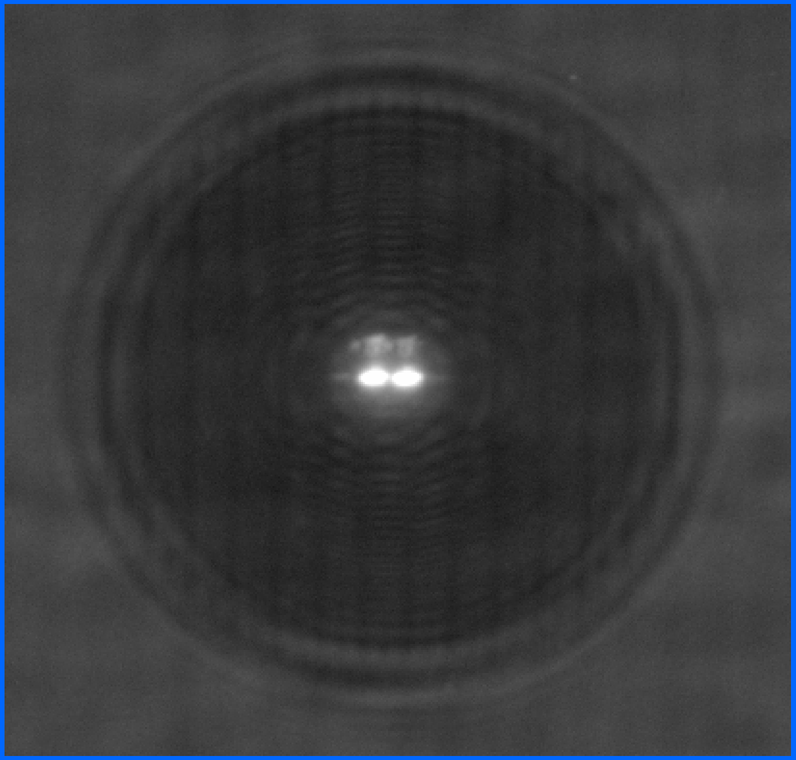

Fine alignment with 50 nm step

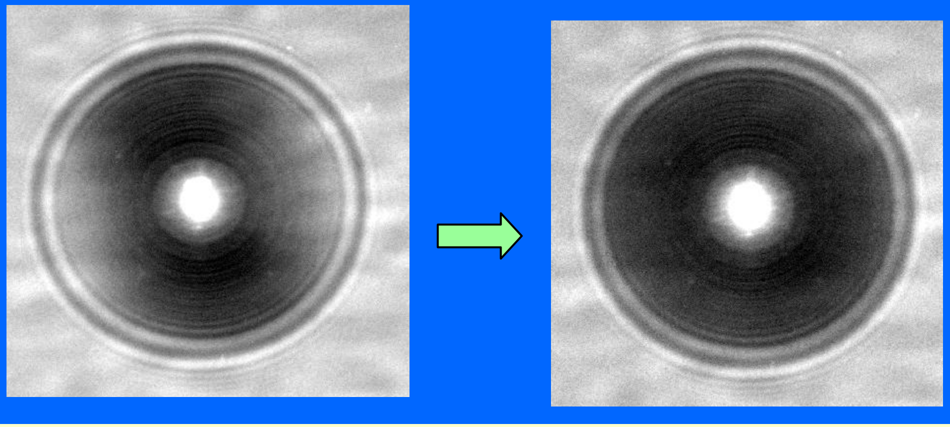

$\Delta r_n/3$

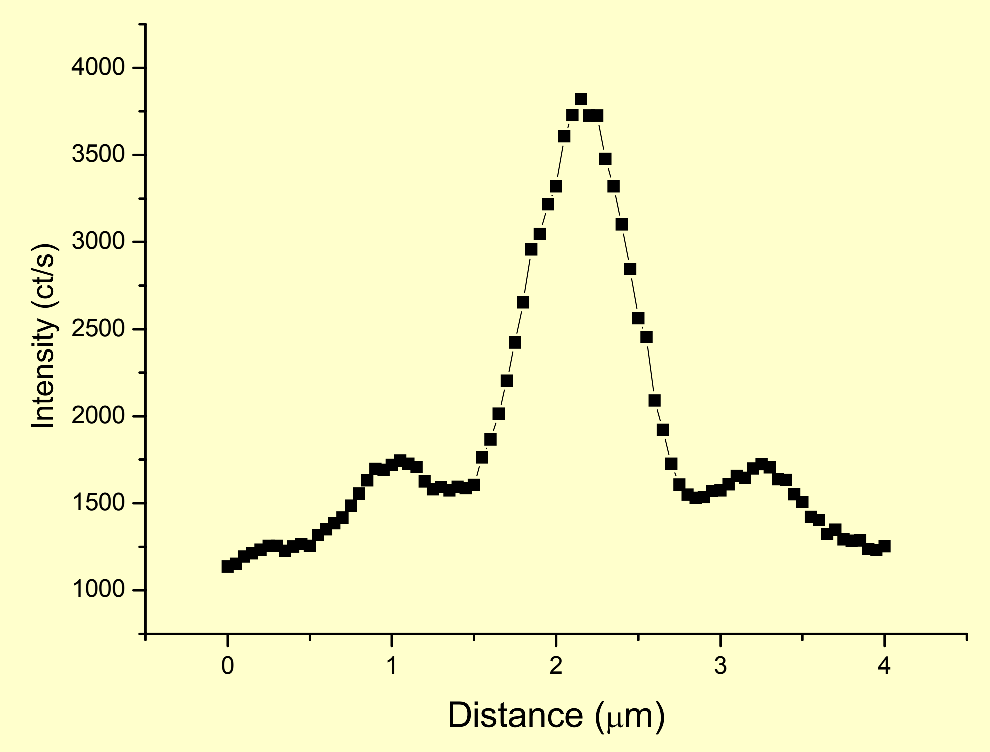

On-line FZP stacking

Tilt compensation for linear displacement

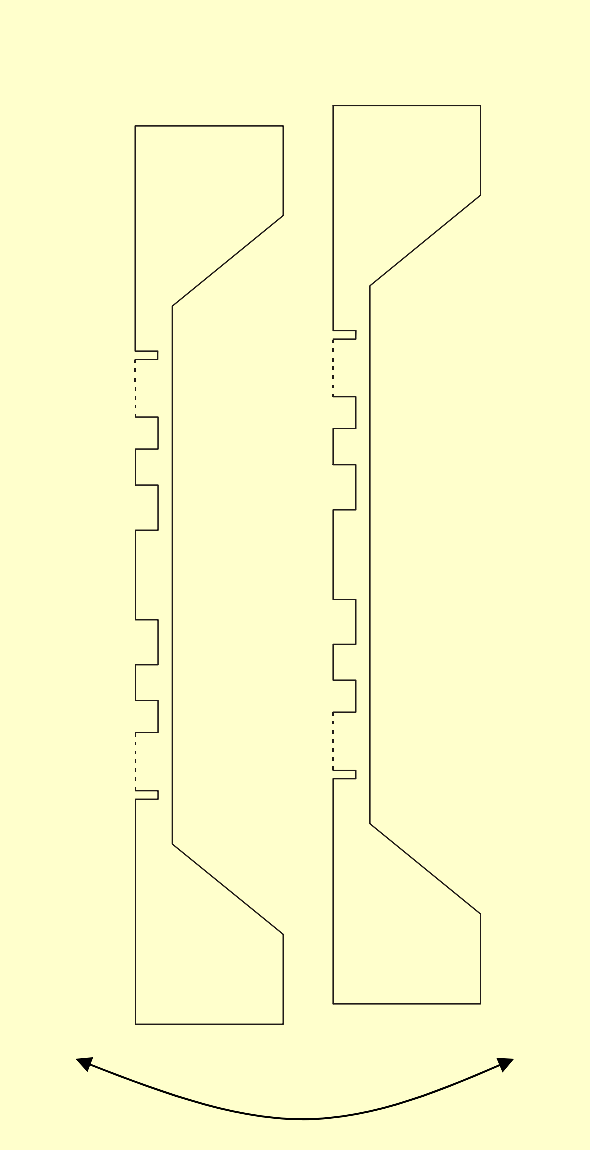

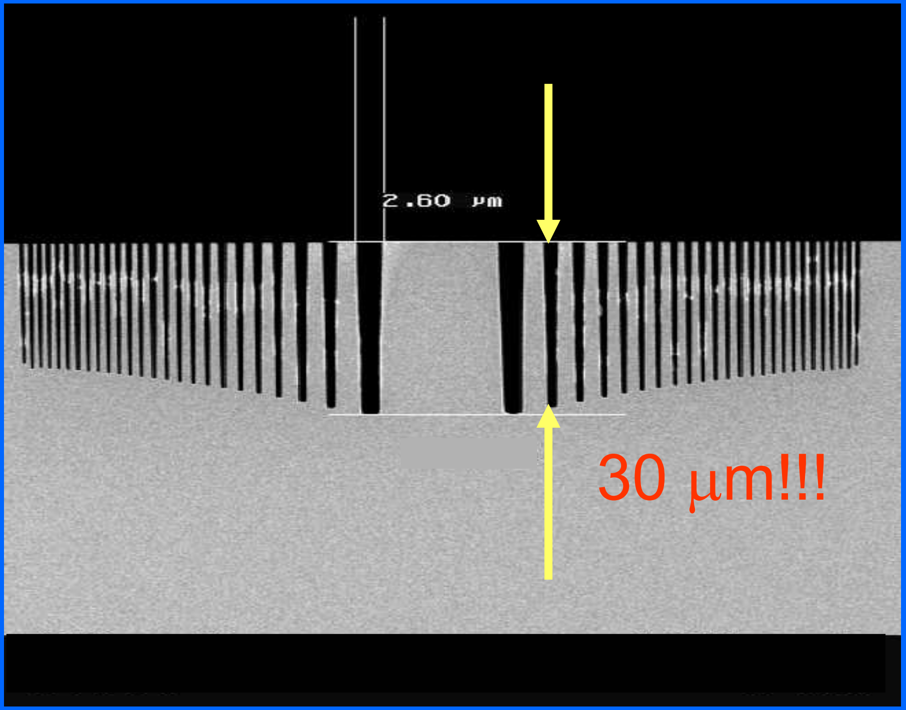

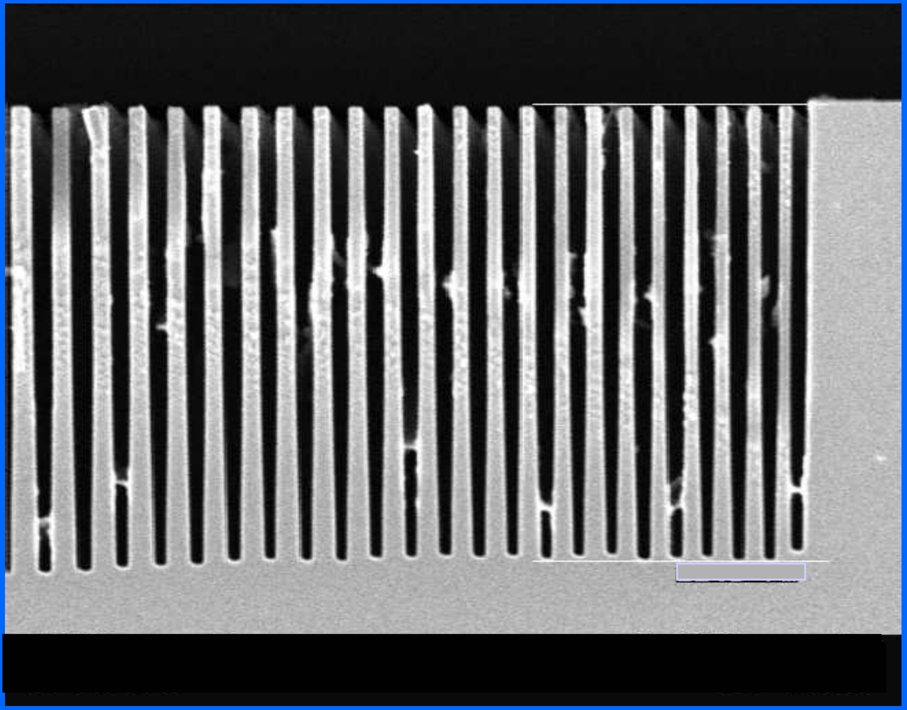

E = 24 keV
eff ~ 30%

2FZP at 50 keV
eff ~ 35%
tested at ID15
F = 3 m

50 keV X-ray focusing with two-stacked FZPs

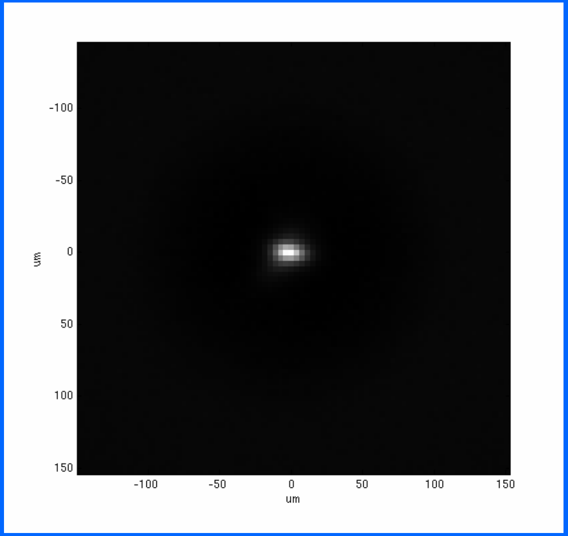

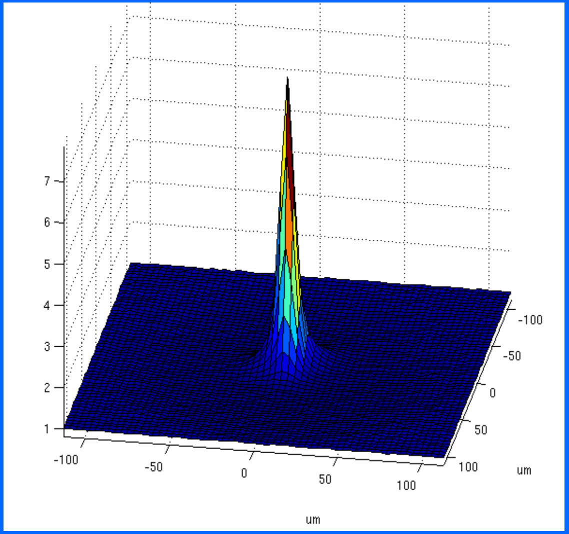

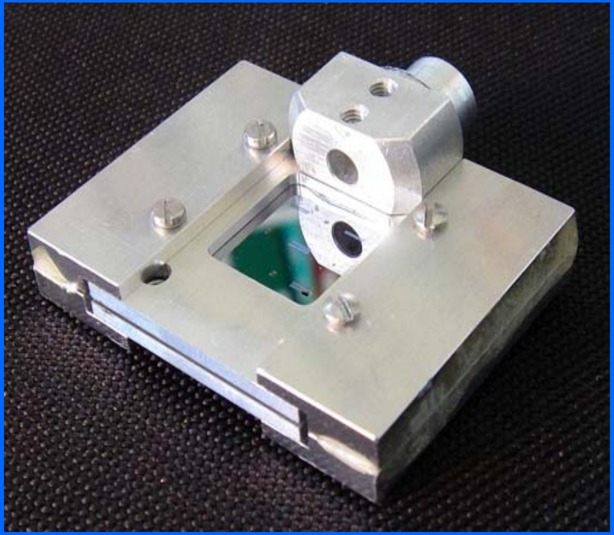

Vertical scan

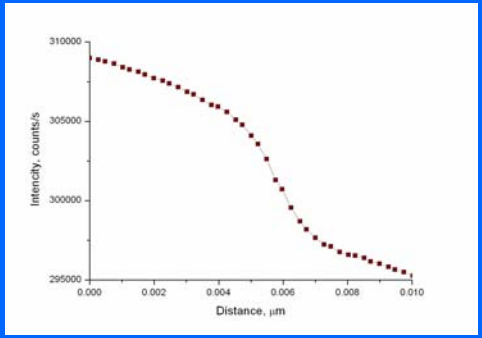

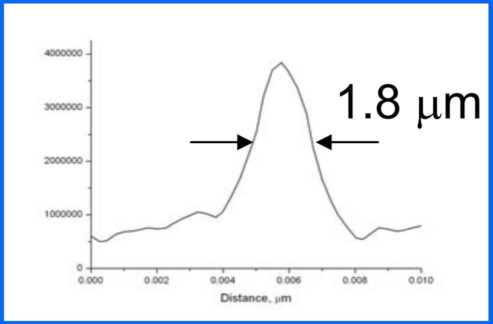

2xFZP DOE7/33
E = 50 keV
L_1 = 60m
L_2 = 3.2 m
A = 200 µm

Gain=450

Spatial resolution limit

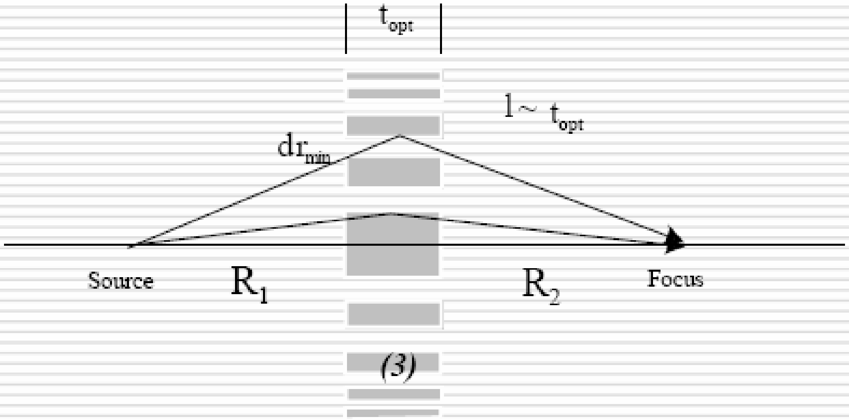

Transmission zone plate

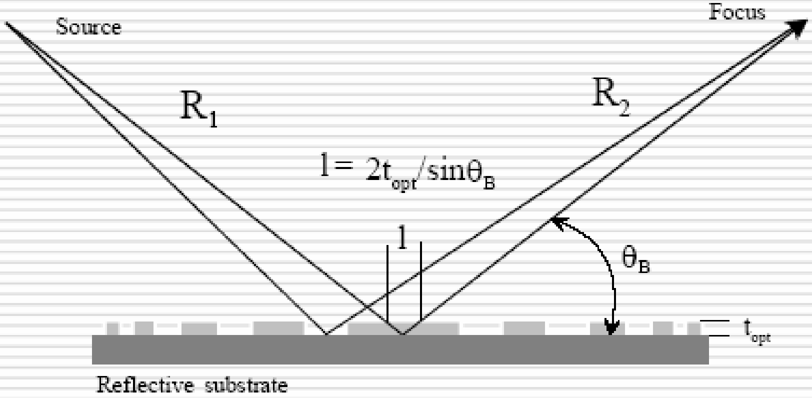

Reflection zone plate

$$\delta r_{\min} > \sqrt{m\lambda t_{opt}}$$

Microfabrication techniques for planar CRLs

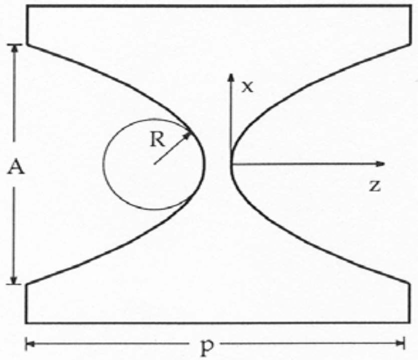

Single parabolic refractive lens

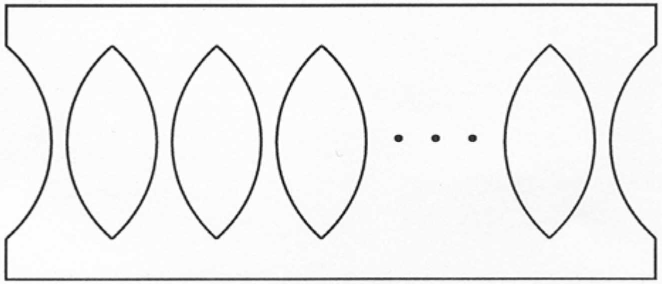

CRL with parabolically shaped holes

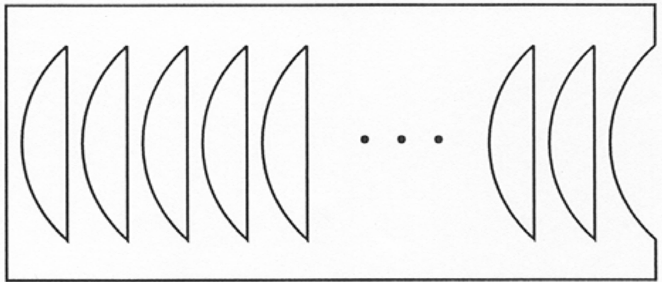

CRL with parabolically shaped half-holes

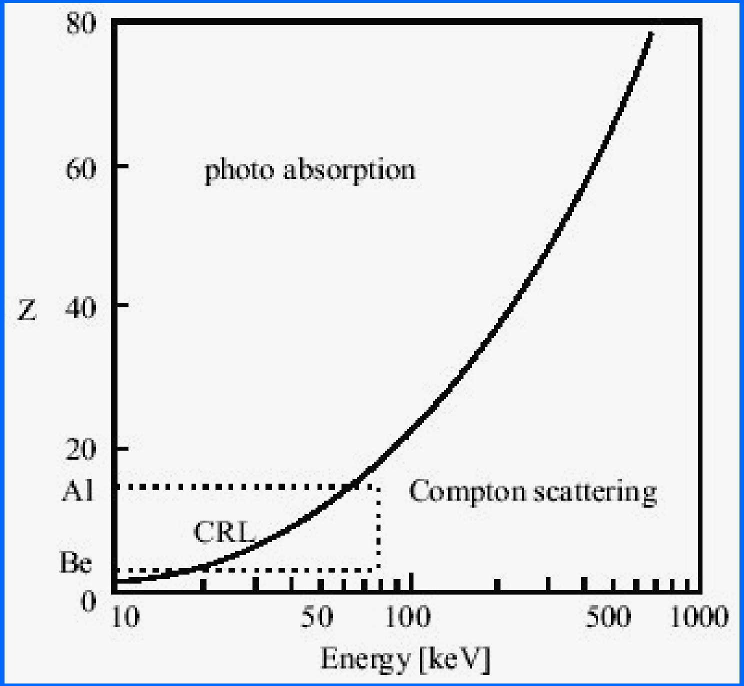

- R must be small R < 0.5 mm
- $\mu/\rho \sim Z^3/E^3$ must be small

  low Z material: Li , Be , B , C , SU-8 , Al, Si
- gain ~ δ/β

	E, keV	δ	β	δ/β
Si	10	4.9E-6	7.4E-8	70
	20	1.2E-6	4.6E-9	250
Diamond	10	7.3E-6	6.9E-9	1000
	20	1.8E-6	3.6E-10	5000

A. Snigirev, V. Kohn, I. Snigireva, A. Souvorov, B. Lengeler, *Applied Optics, vol. 37, 653, 1998.*

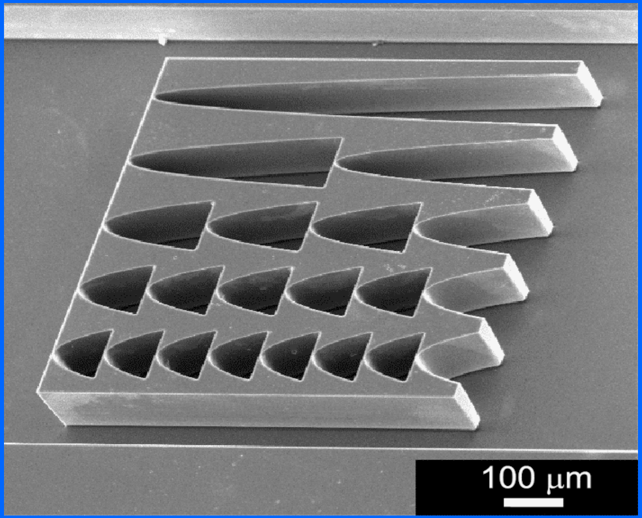
100 µm

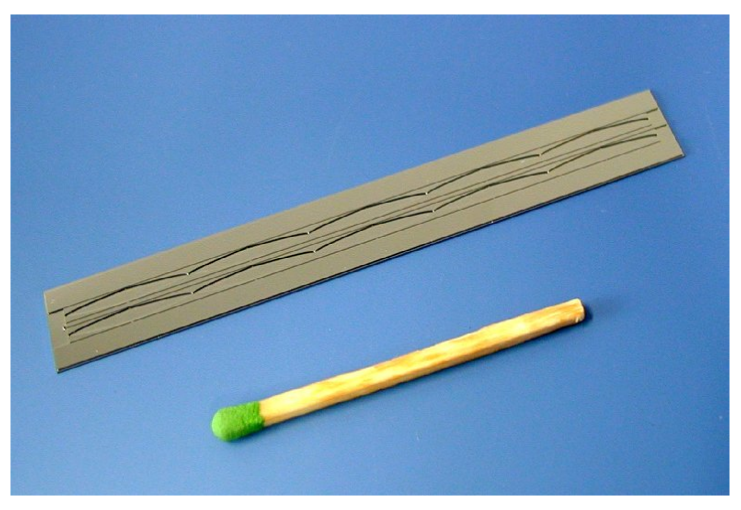

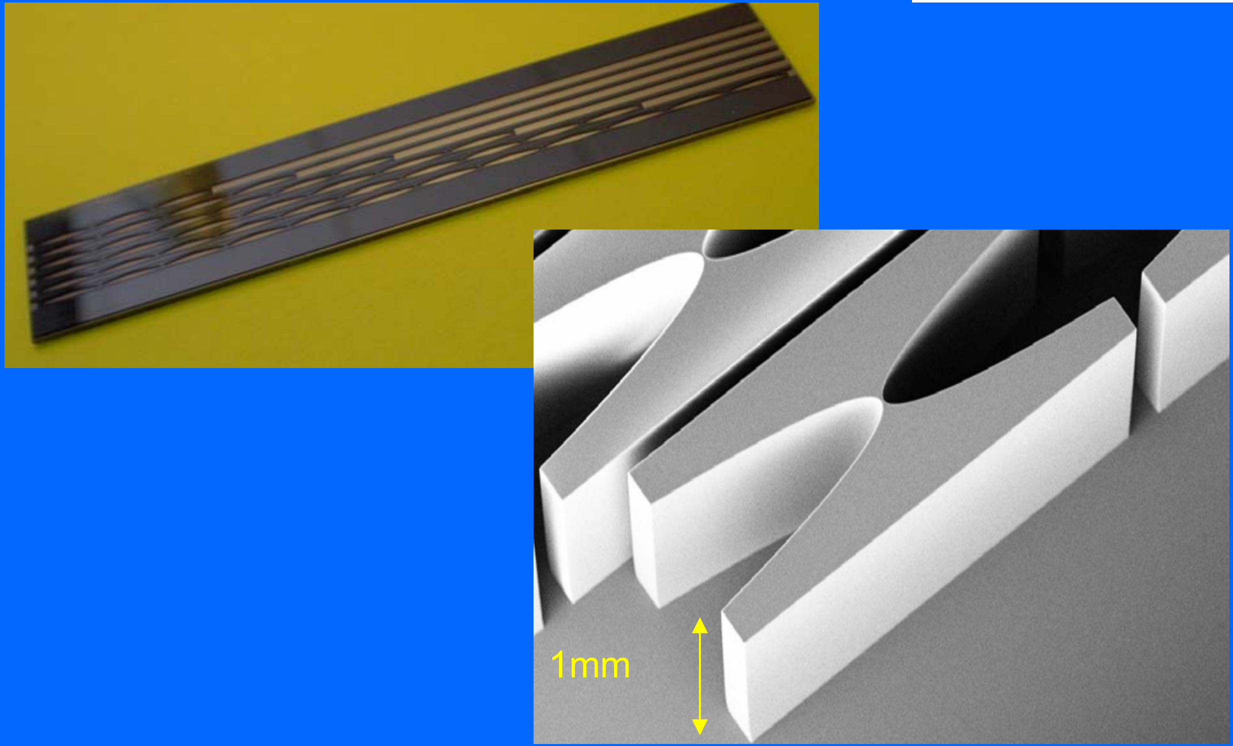
1mm

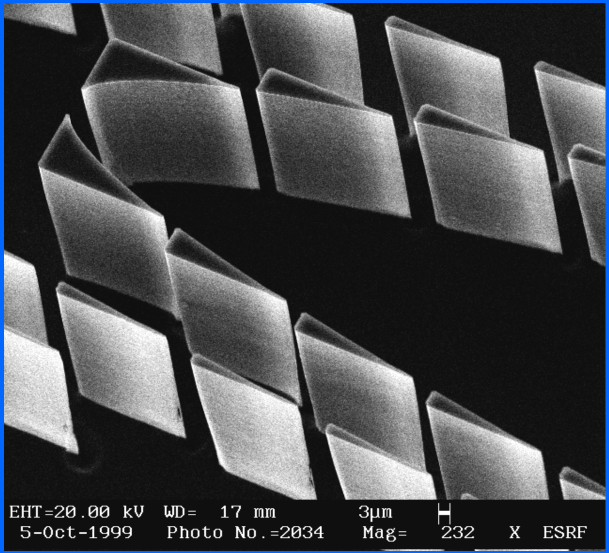
EHT=20.00 kV
WD= 17 mm
3µm
5-Oct-1999
Photo No.=2034
Mag= 232 X
ESRF

Advantages of micro-fabrication technology

- Any combination of refraction and diffraction properties
- Computer-aided design (from incident wavefront correction to pre determined exit wavefront generation)
- No diffraction-limited aperture
- Use of low-*Z* materials that are hard for machining (Si, B, diamond)

Advantages of Linear focusing

- Astigmatic focusing

  vertical source size is smaller then horizontal one.
- Combination with other BL focusing elements as crystals, mirrors.
- Needs for high resolution diffraction and scattering techniques including surface analysis, high resolution diffraction experiments, standing waves technique

Si lenses with 0.3 – 0.4 μm profile deviation

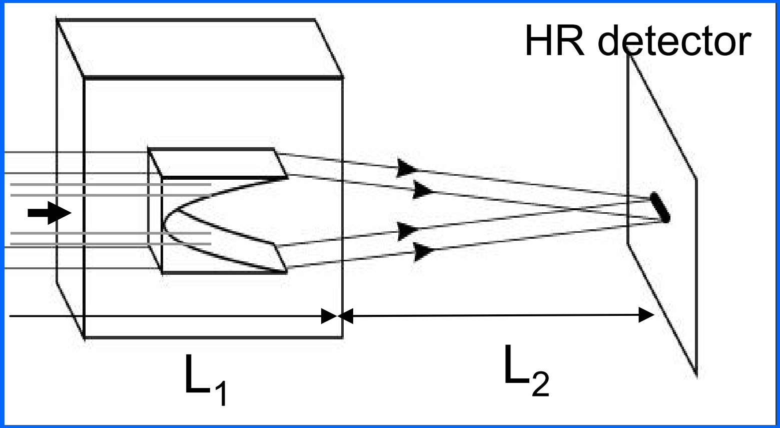

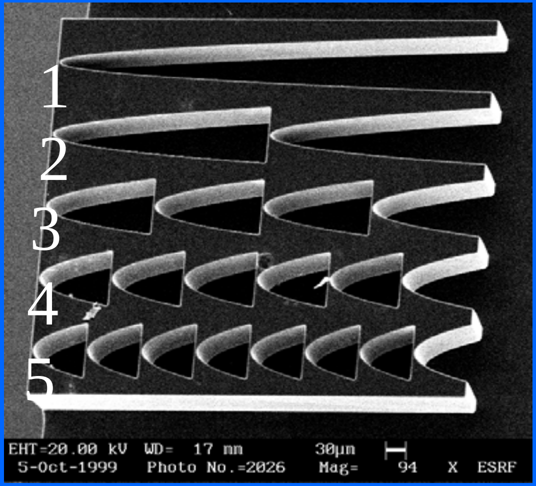

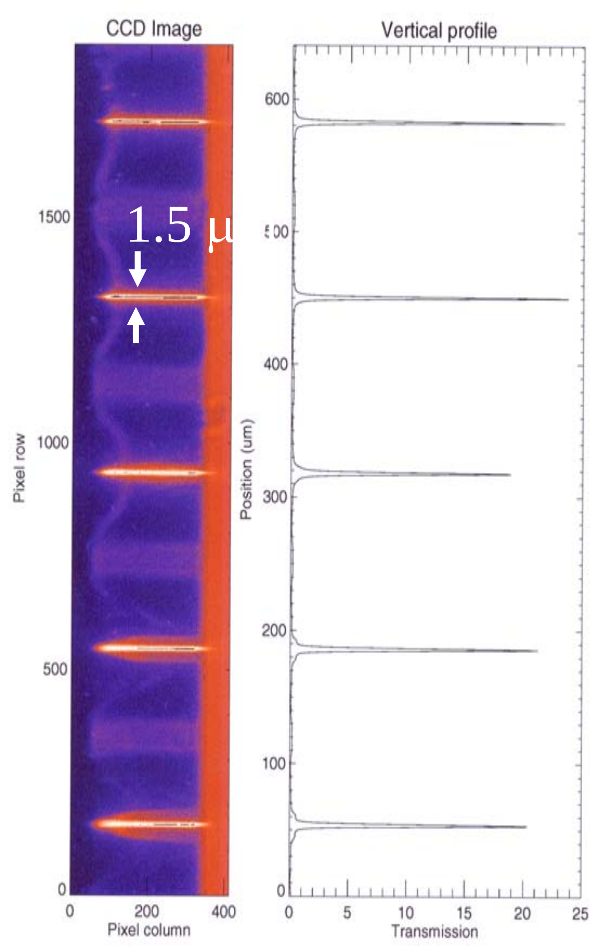

aperture	100 μm
hight	100 μm
web size	5 μm

lens $R_{\text{parabola tip}}$

1 - 3.2 μm;
2 - 6.4 μm;
3 - 12.8 μm;
4 - 19.1 μm;
5 - 25.4 μm

E = 14 keV

F = 75 cm

Source size 30 μm

Source-to-lens distance 60 m

FWHM = 1.5 μm

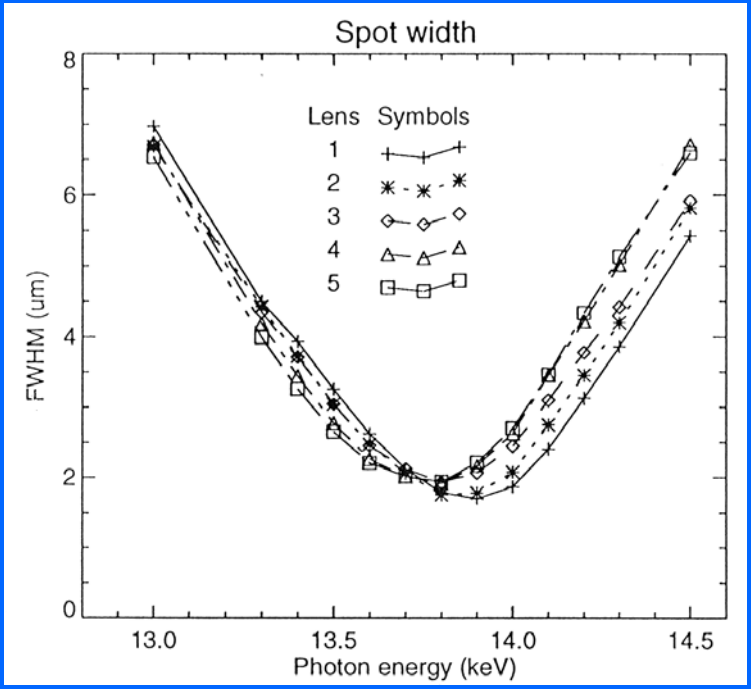

Focus depth energy scan for 5 lenses

Test of Si lenses with 0.3 – 0.4 μm profile deviation at SPRing-8

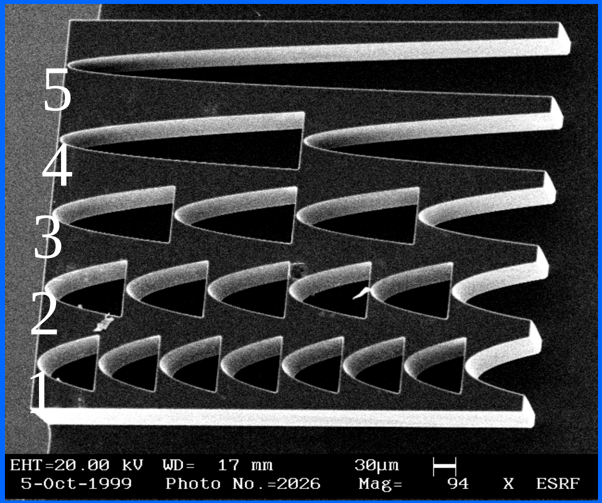

E = 17 keV F = 100 cm
Source size 15 μm
Source-to-lens distance 1 km !!!
FWHM = 0.9 μm

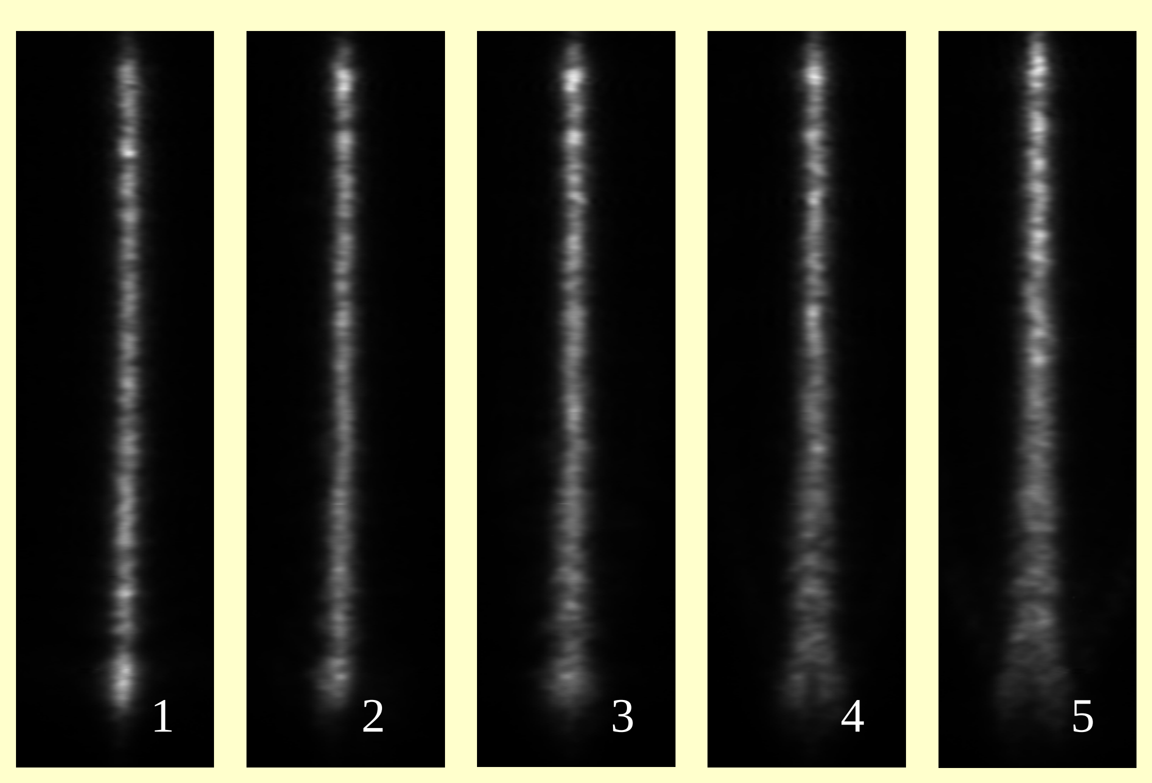

Detector resolution
0.3 μm

A. Souvorov et al

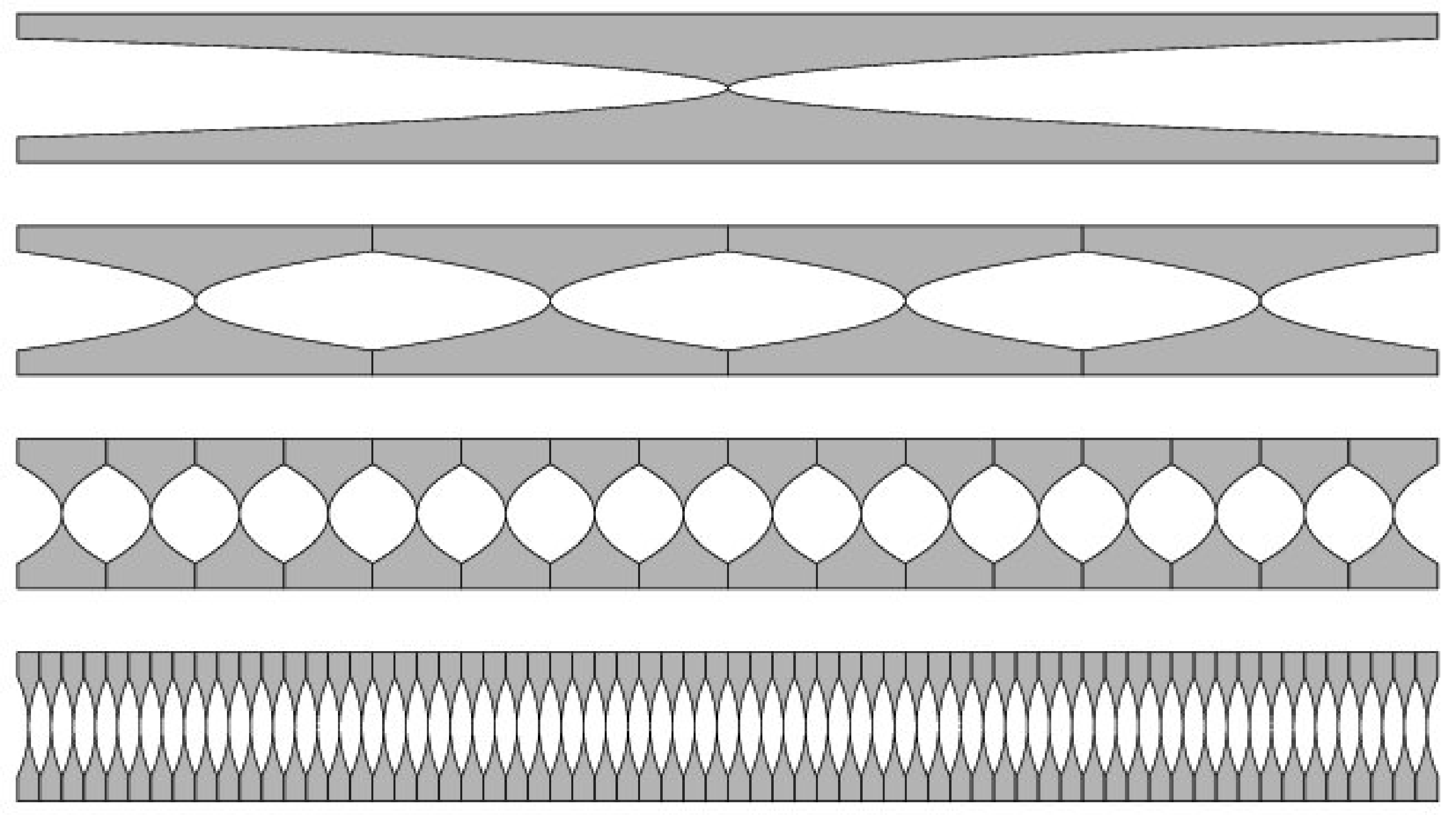

$$F = \frac{R}{2N\delta}$$

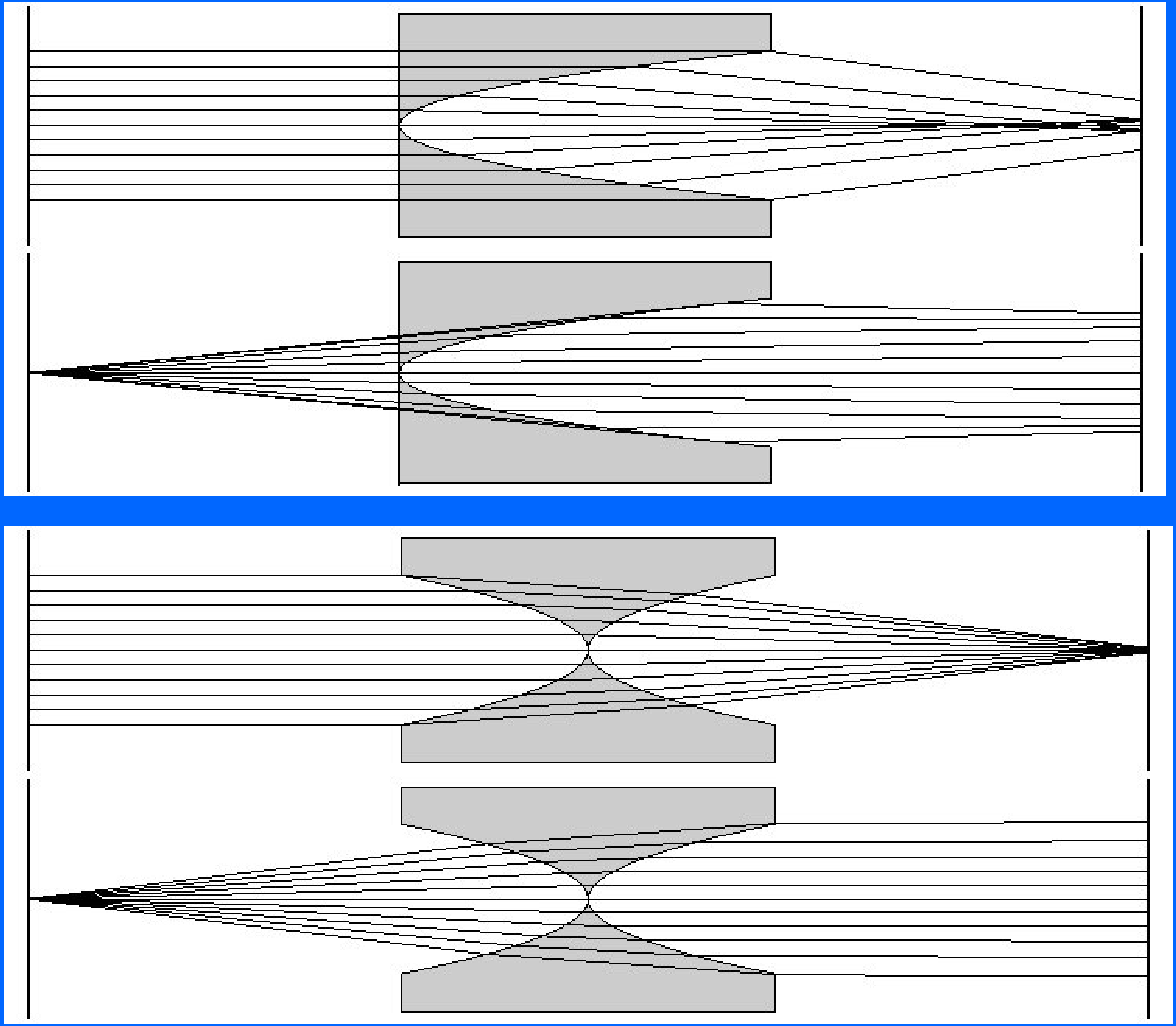

Fabrication of silicon parabolic lenses

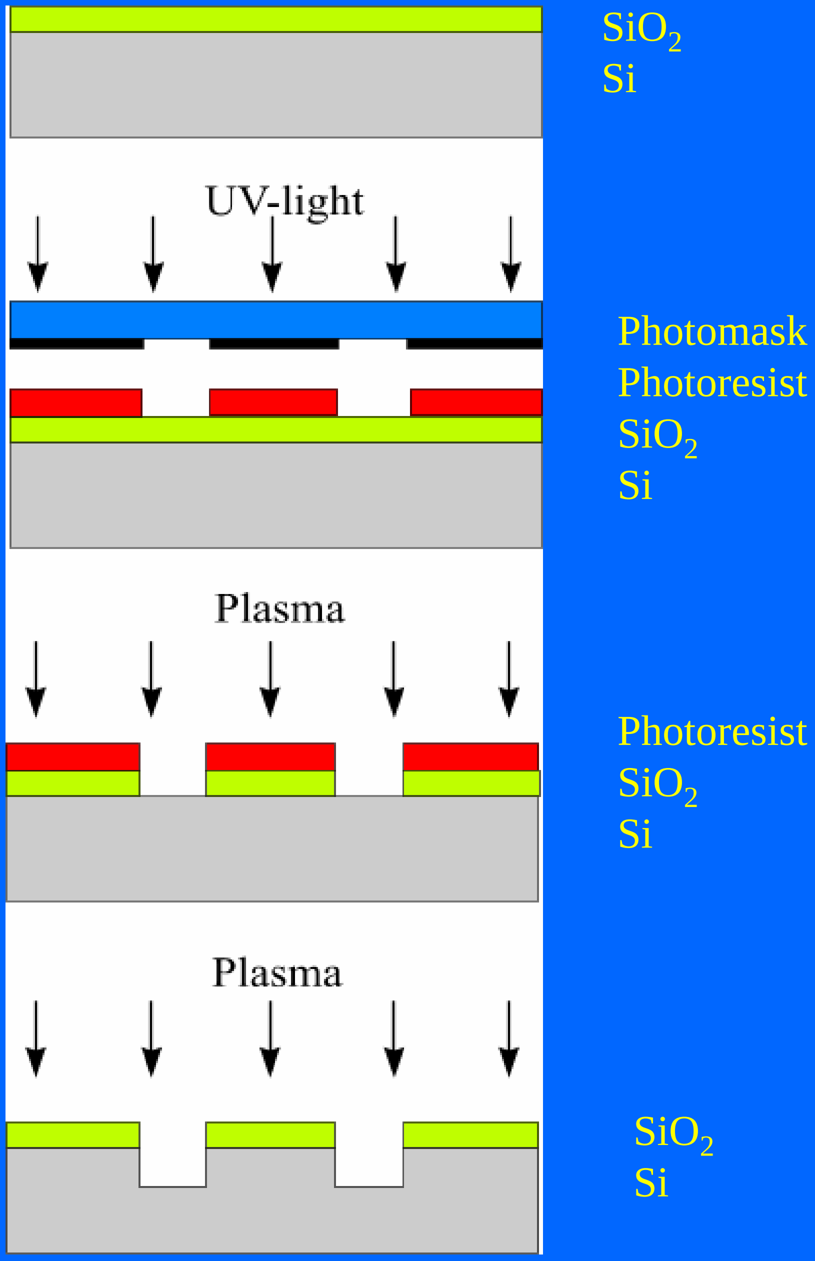

Thermal oxidation of Si wafer

Resist spin, exposure and development

Anisotropic oxide etching in CHF_3 plasma

Deep silicon etching in “Bosch process”

Inaccuracies in deep silicon etching

Etched depth and shape of trenches depend on aspect ration and/or trench width

- **1 mm-**wide trenches have negatively sloped sidewalls
- **20 µm** trench exhibits nearly vertical profile

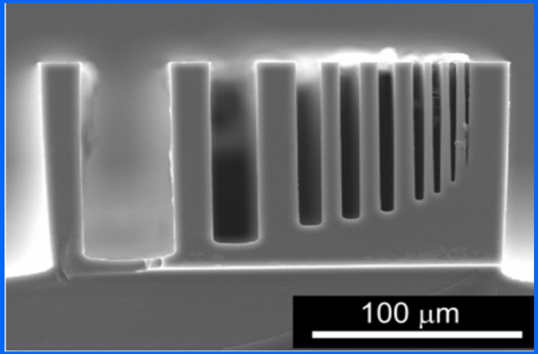

Mask undercut is:

- in the range of **0.5-0.6 µm**
- independent on the trench width

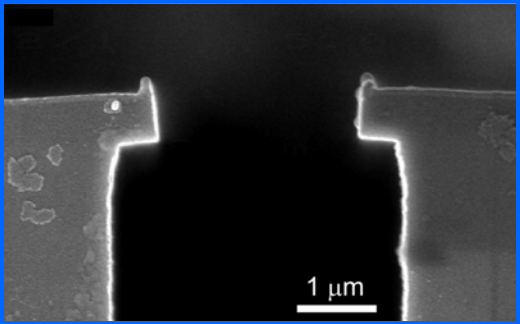

Deviation of the parabolic refractive profile from the ideal one caused by mask undercut and sidewall etching during silicon etching down to **200 µm**

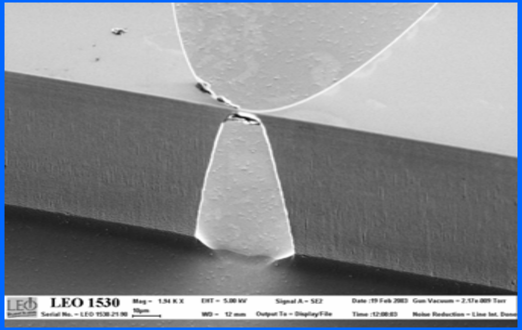

Parabola approximation

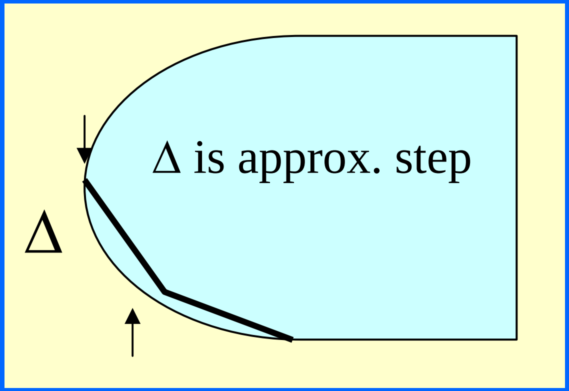

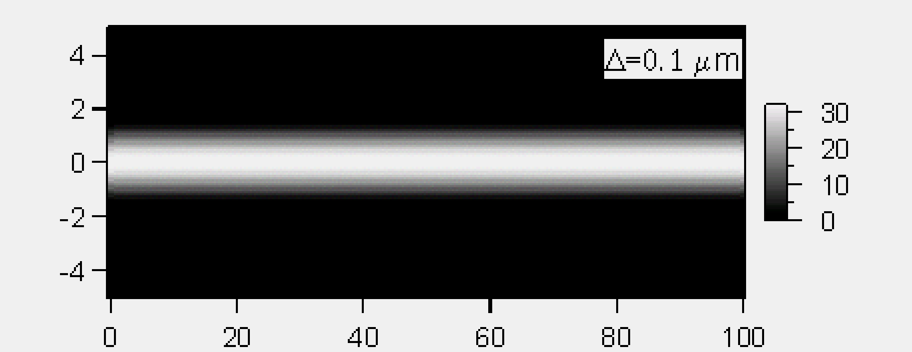

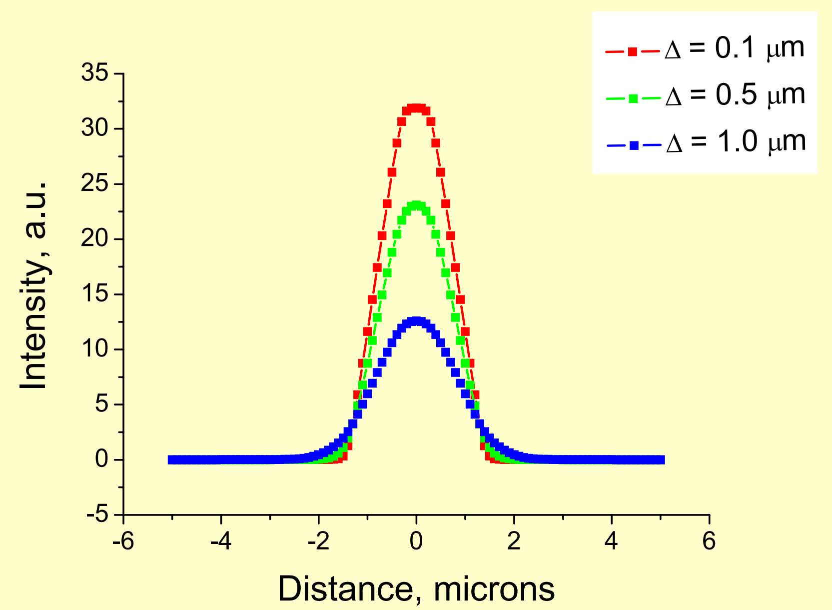

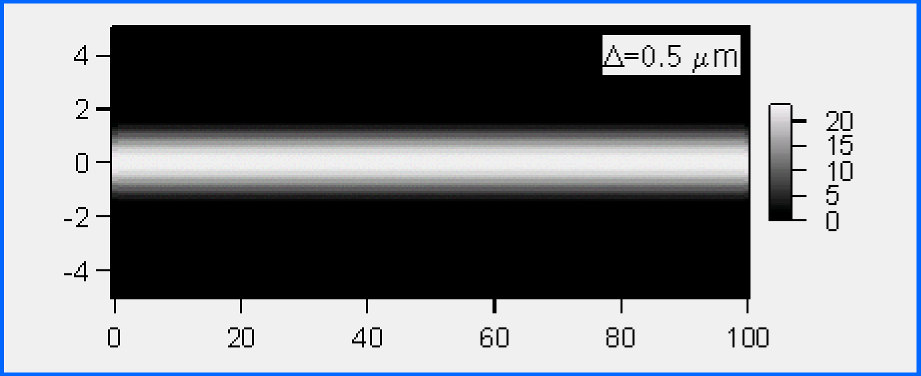

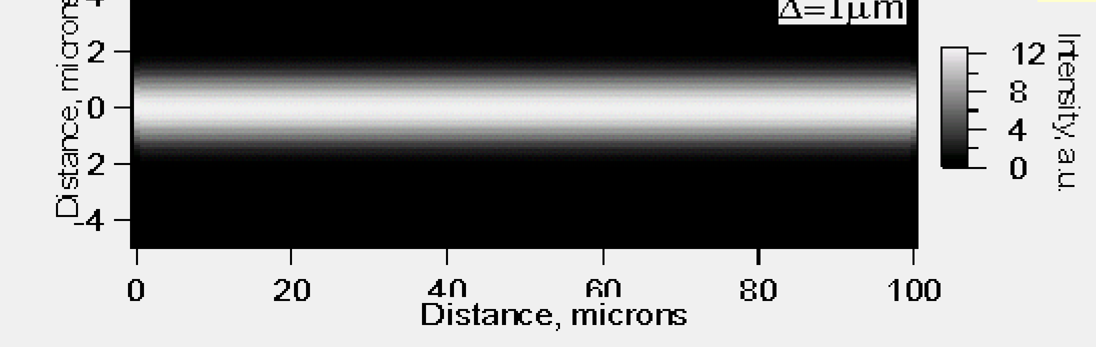

optimization of parabolic profile approximation is compromise between a precise parabola and a size of data file for lithography.

Profile deviations: experiment and simulation

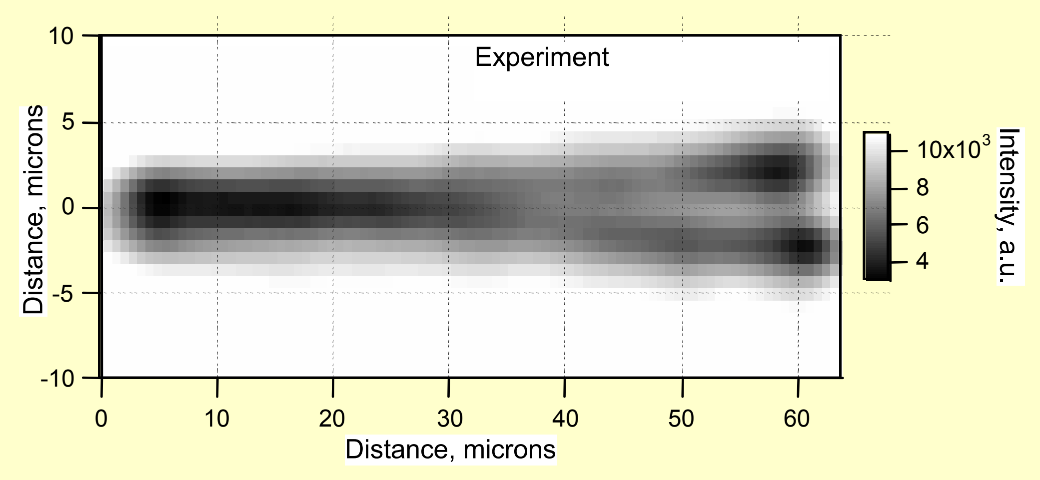

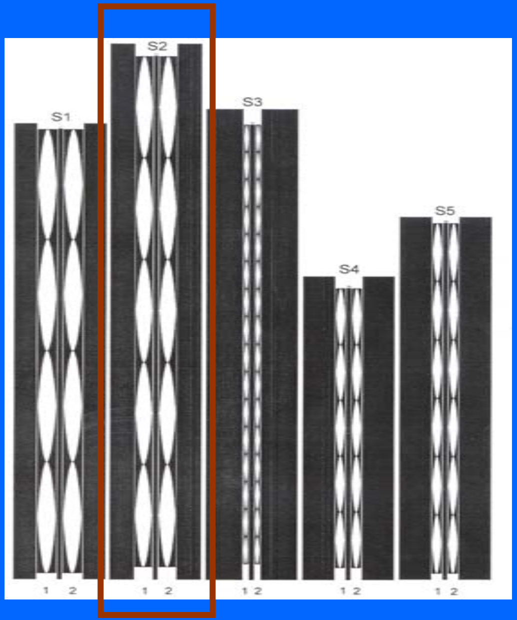

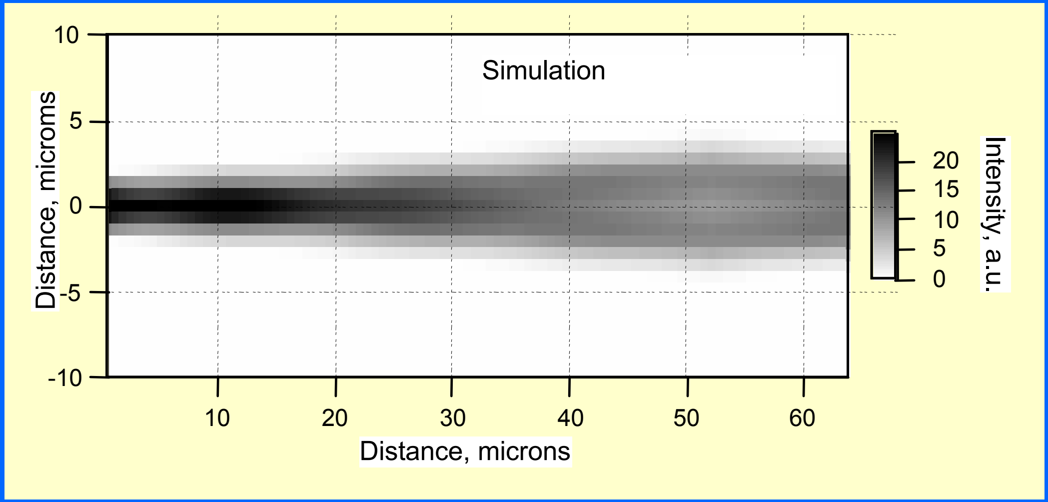

3.5µm tolerance

E= 20 keV

F= 40 cm

A= 500 µm

N= 32

Lens-to-detector distance 43 cm

Test of Energy-Tunable Si-lens

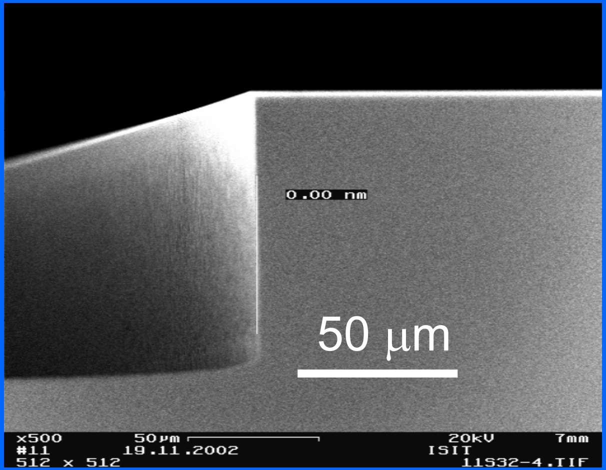

52 mm

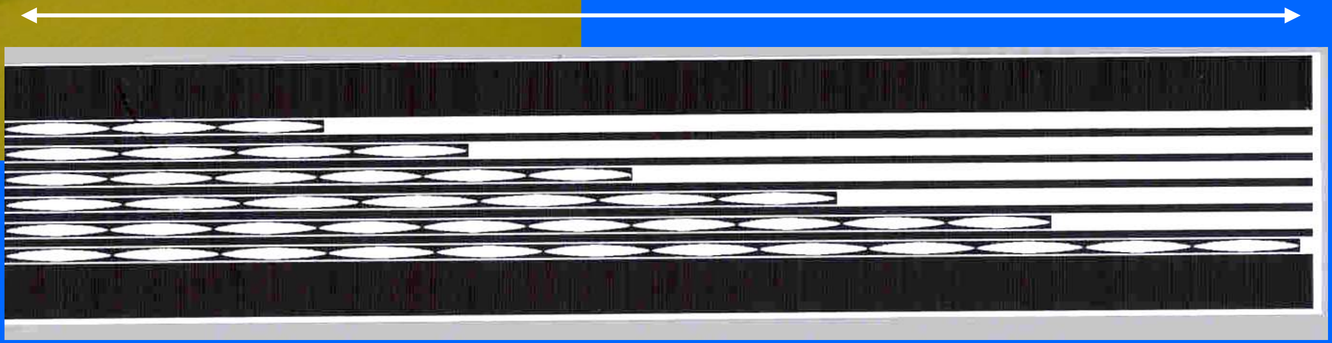

Lens number	Energy, keV	Number of lenses, 2N	Lens length, cm	Aperture, µm	Focal spot, µm	Focal distance, cm
S6 - 1	10	6	1.28	500	3.6	50.4
S6 - 2	12	8	1.86	500	3.7	51.1
S6 - 3	14	12	2.51	500	3.6	50.8
S6 - 4	16	14	3.33	500	3.7	50.1
S6 - 5	18	20	4.18	500	3.9	50.5
S6 - 6	20	24	5.17	500	3.6	51

Long BL: 100m
Source 50μm x 150μm

F = 10 cm
50 nm x 150 nm
Demagnification X 1000

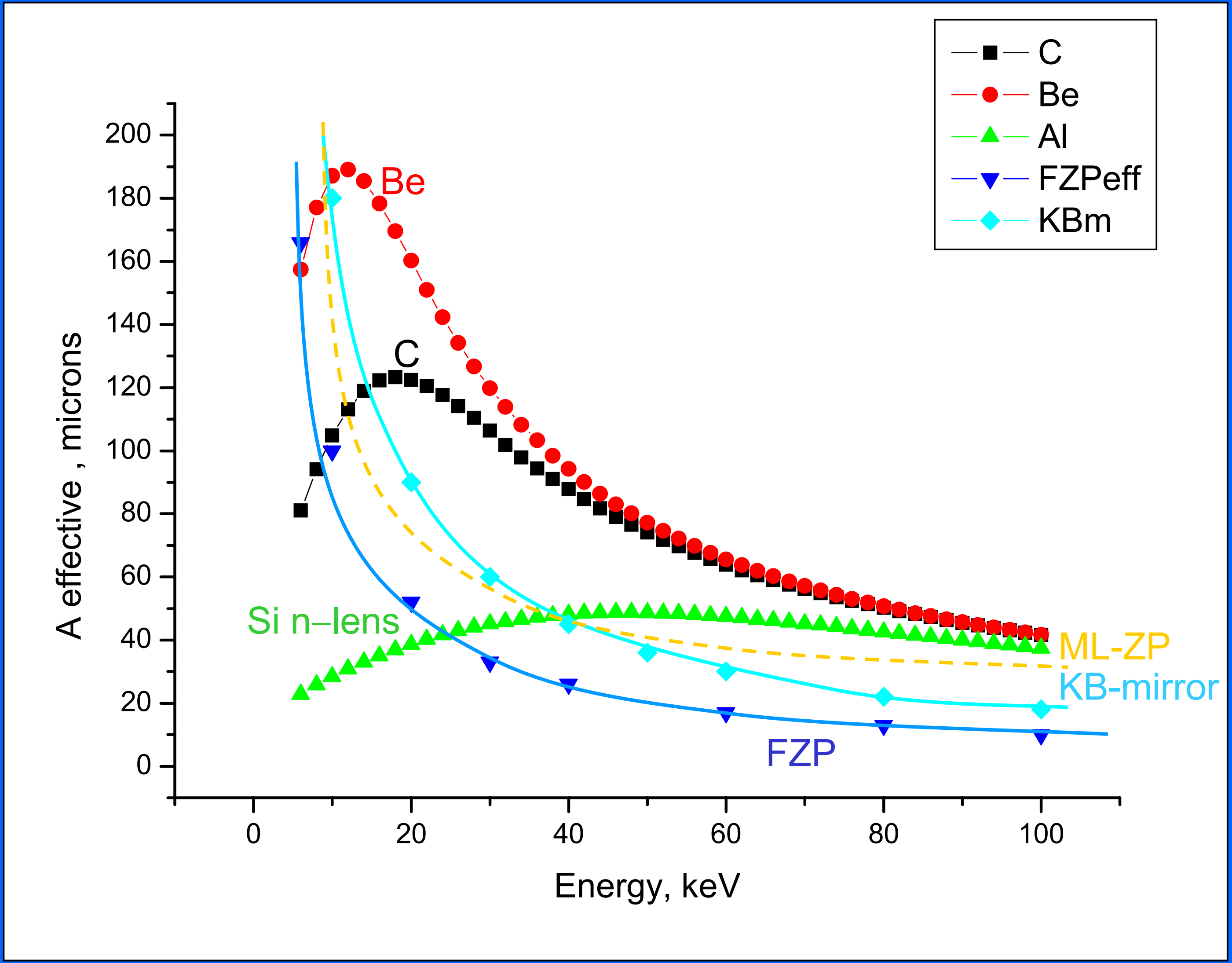

Lens chip design

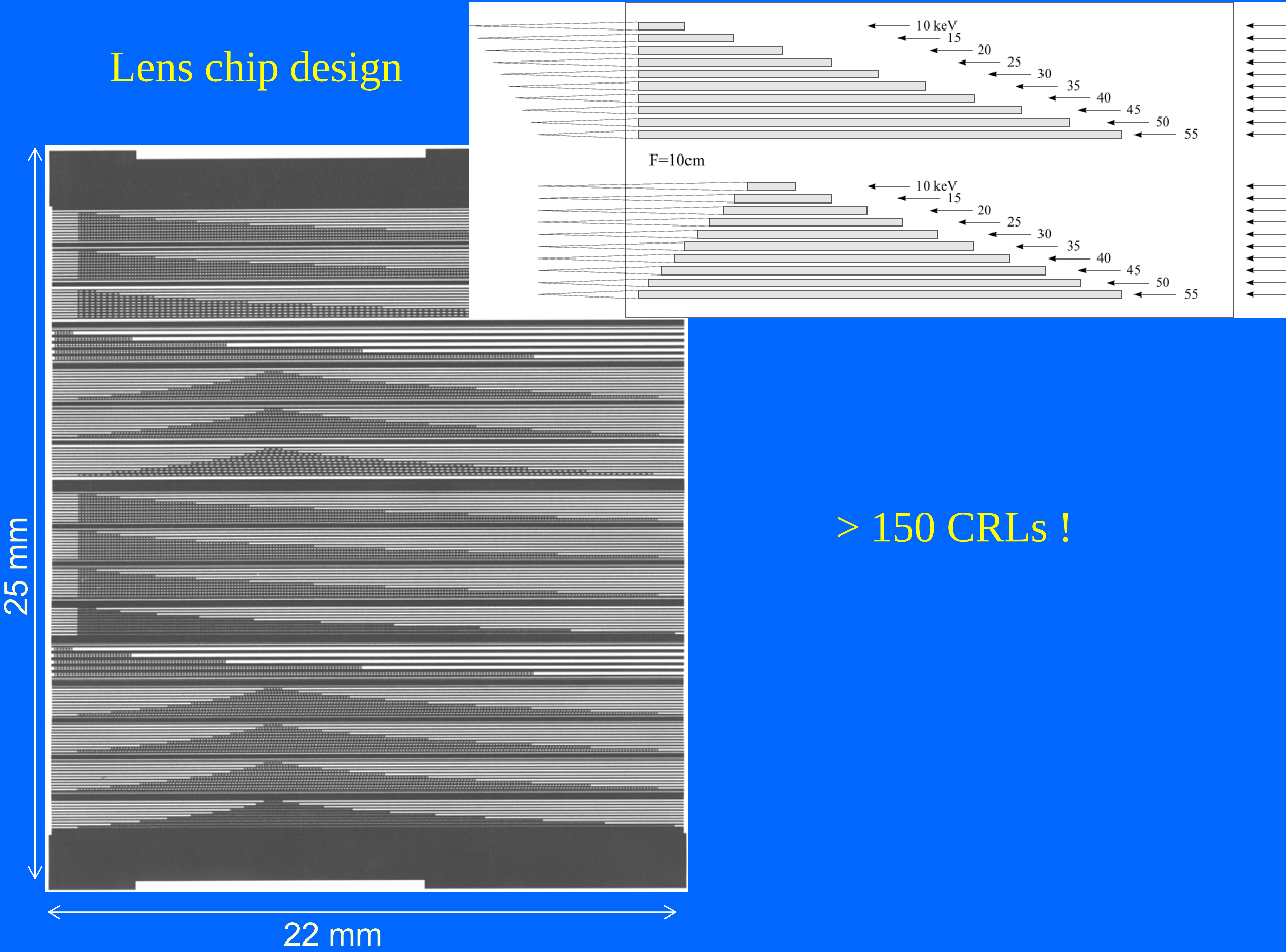

> 150 CRLs !

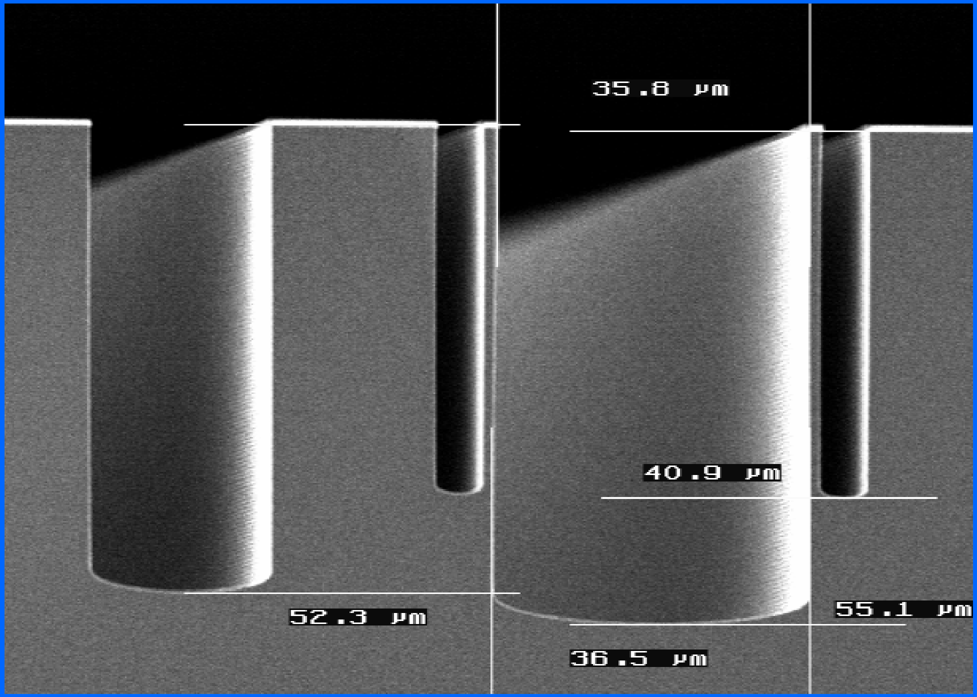
35.8 μm
40.9 μm
52.3 μm
55.1 μm
36.5 μm

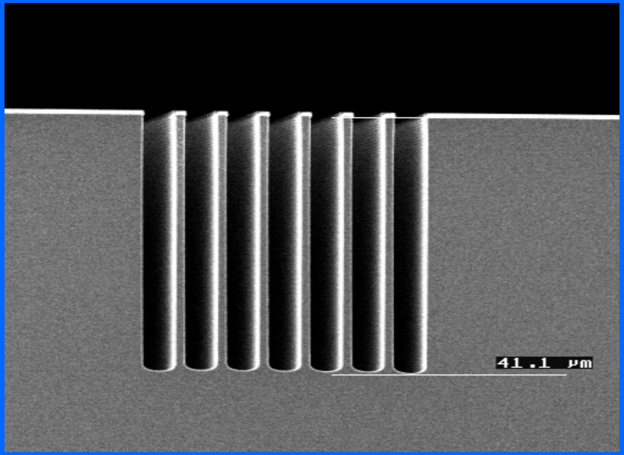
41.1 μm

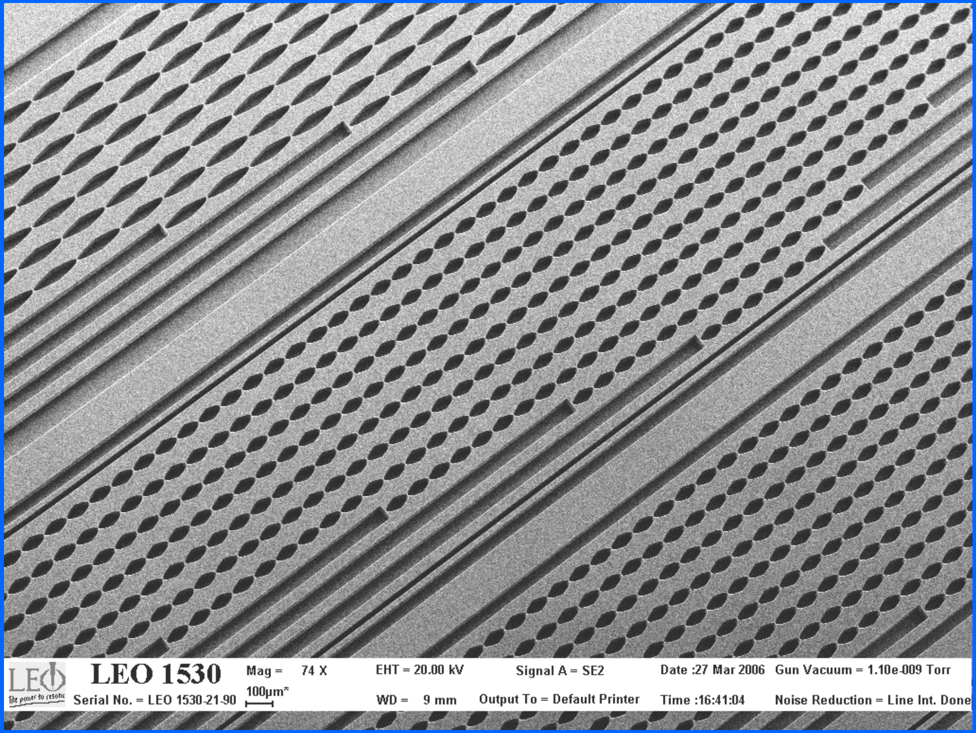
LEO 1530
Serial No. = LEO 1530-21-90
Mag = 74 X
100µm*
EHT = 20.00 kV
WD = 9 mm
Signal A = SE2
Output To = Default Printer
Date :27 Mar 2006
Time :16:41:04
Gun Vacuum = 1.10e-009 Torr
Noise Reduction = Line Int. Done

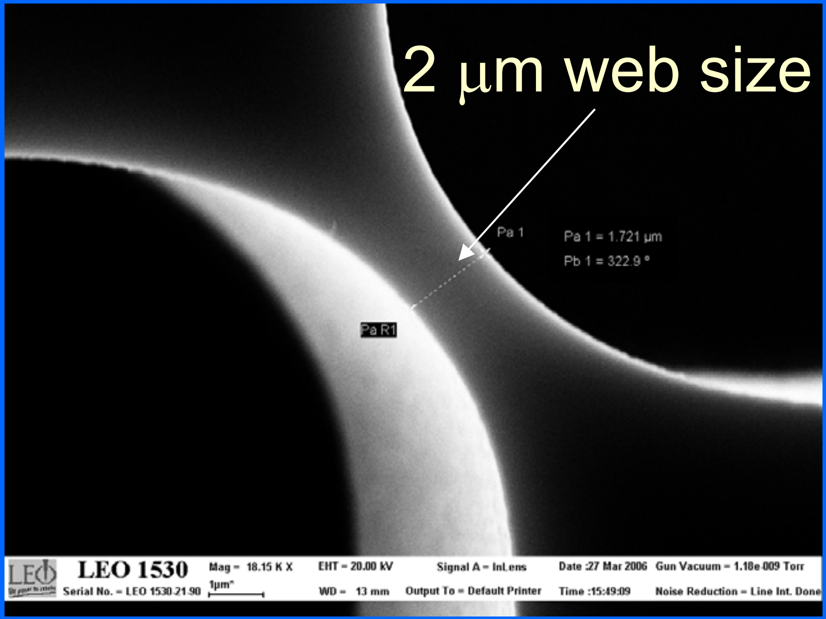
2 µm web size
Pa 1
Pa 1 = 1.721 µm
Pb 1 = 322.9 °
Pa R1
LEO 1530
Serial No. = LEO 1530-21-90
Mag = 18.15 K X
1µm*
EHT = 20.00 kV
WD = 13 mm
Signal A = InLens
Output To = Default Printer
Date :27 Mar 2006
Time :15:49:09
Gun Vacuum = 1.10e-009 Torr
Noise Reduction = Line Int. Done

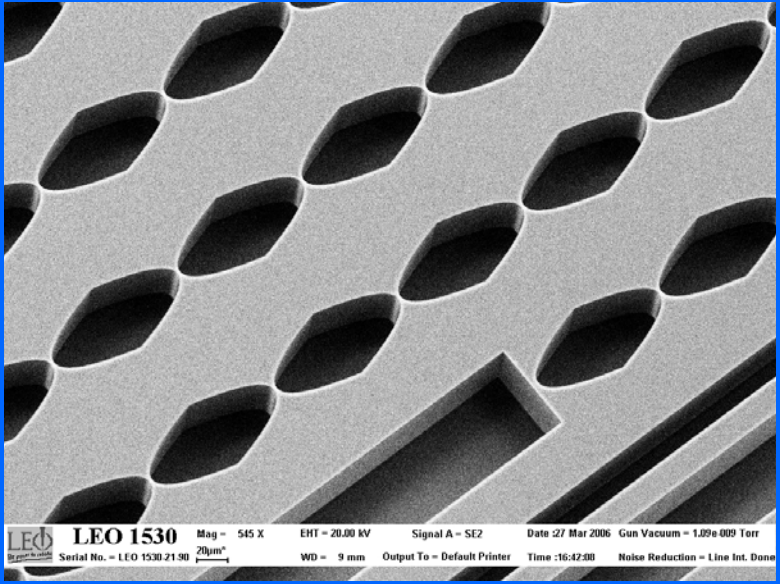
LEO 1530
Serial No. = LEO 1530-21-90
Mag = 545 X
20µm*
EHT = 20.00 kV
WD = 9 mm
Signal A = SE2
Output To = Default Printer
Date :27 Mar 2006
Time :16:42:08
Gun Vacuum = 1.09e-009 Torr
Noise Reduction = Line Int. Done

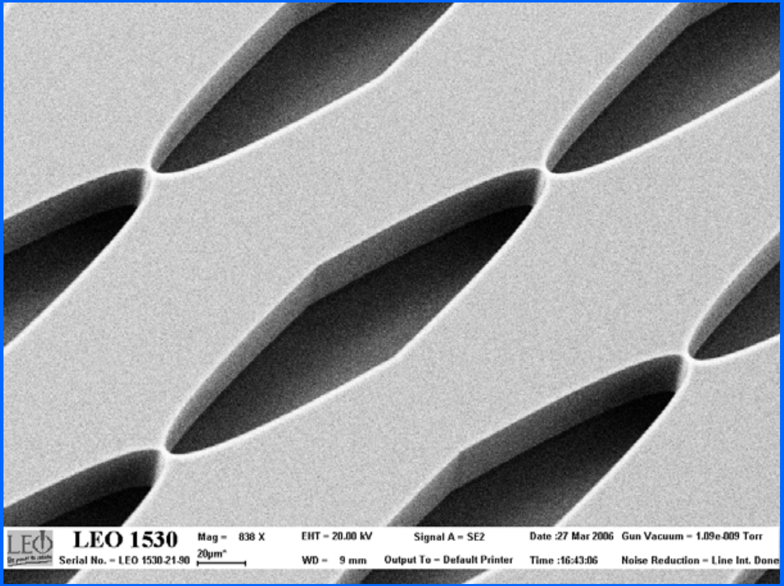
LEO 1530
Serial No. = LEO 1530-21-90
Mag = 838 X
20µm*
EHT = 20.00 kV
WD = 9 mm
Signal A = SE2
Output To = Default Printer
Date :27 Mar 2006
Time :16:43:06
Gun Vacuum = 1.09e-009 Torr
Noise Reduction = Line Int. Done

Test at BM05/MOTB in April 2006

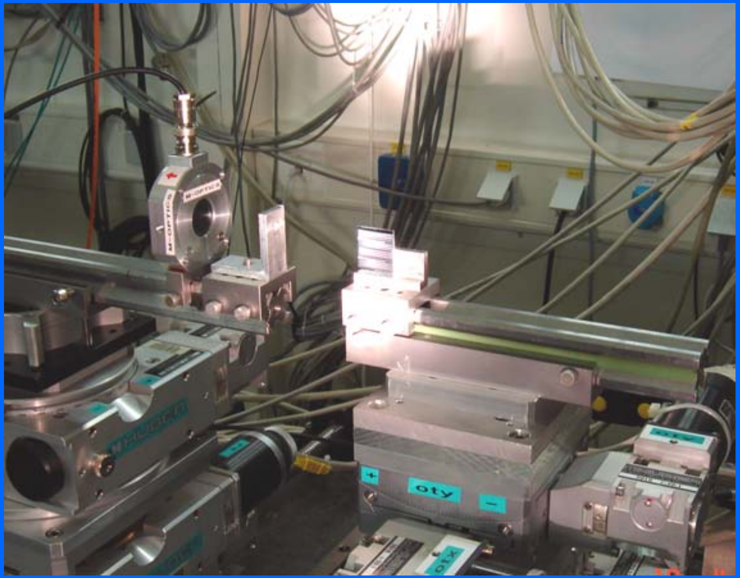

E = 15-30 keV
resolution 200-300 nm

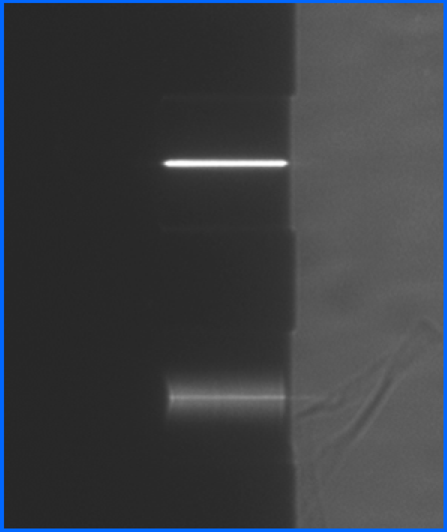

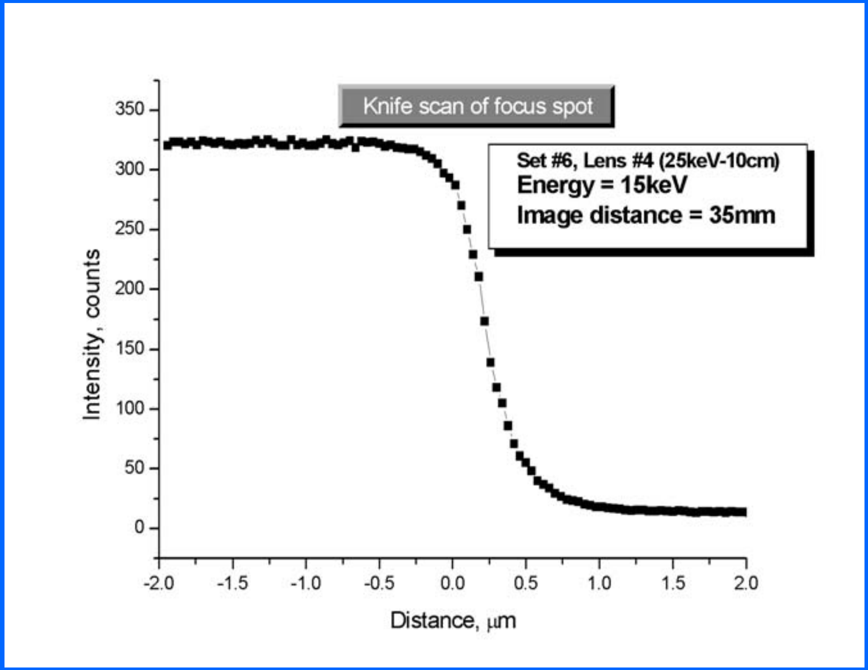

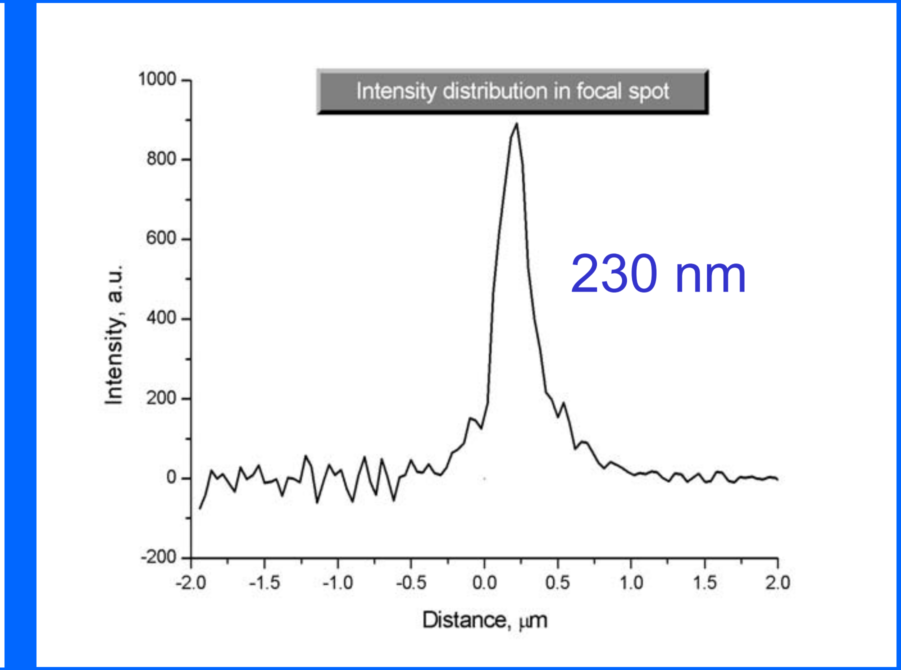

230 nm

Test at ID15 in May 2006

E = 40-80 keV   resolution 200-300 nm

Best: 150 nm at 50 keV!

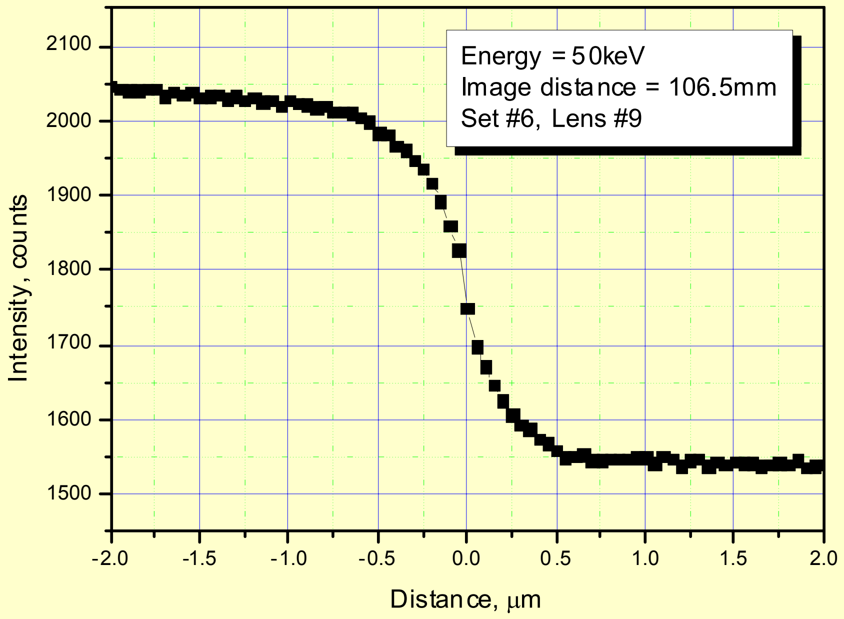

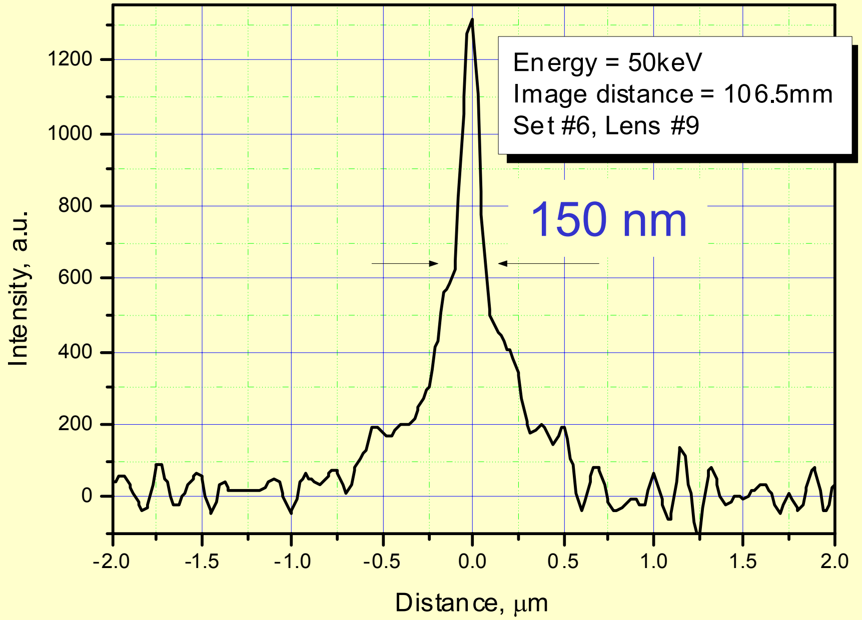

Bi-lens / Billet split lens

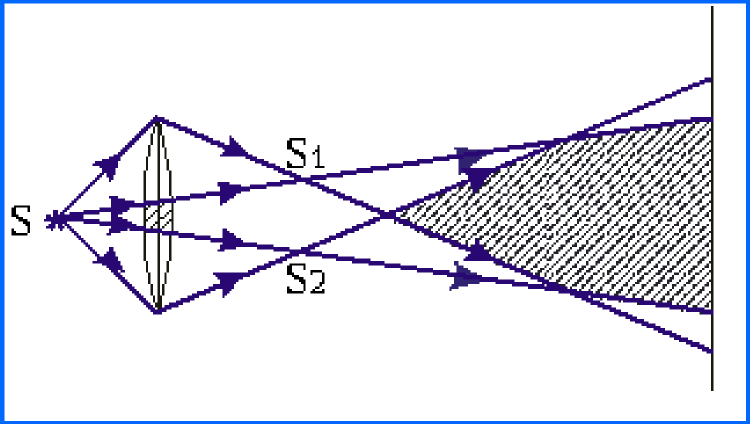

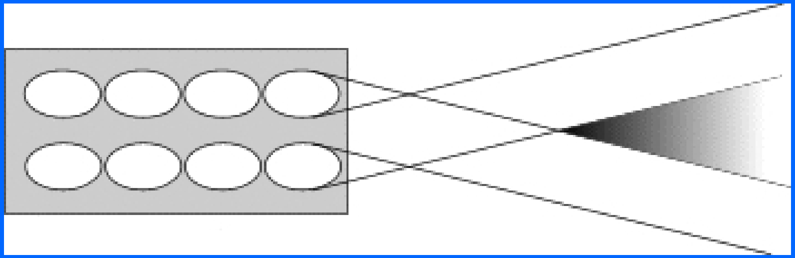

50 - 100 μm ↕

Spatial coherence characterization
MOTB/BM5

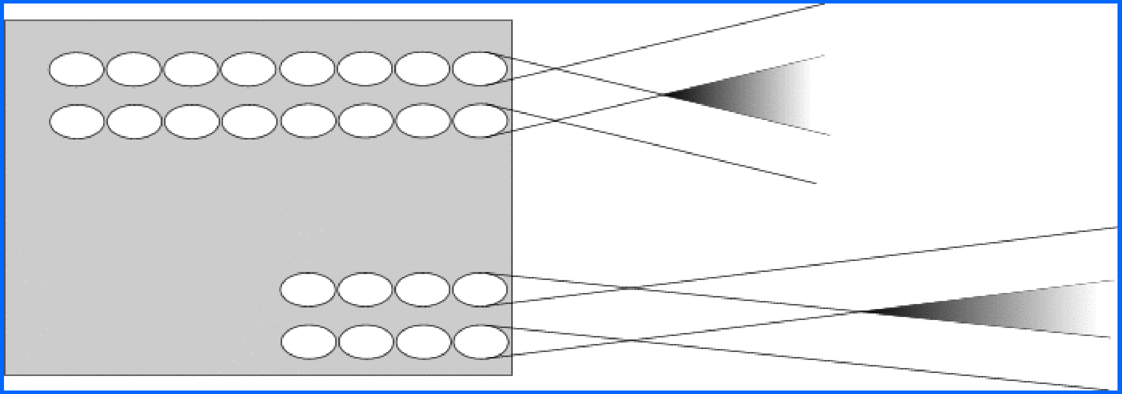

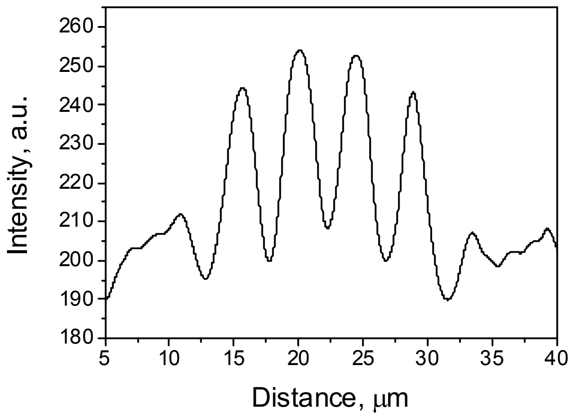

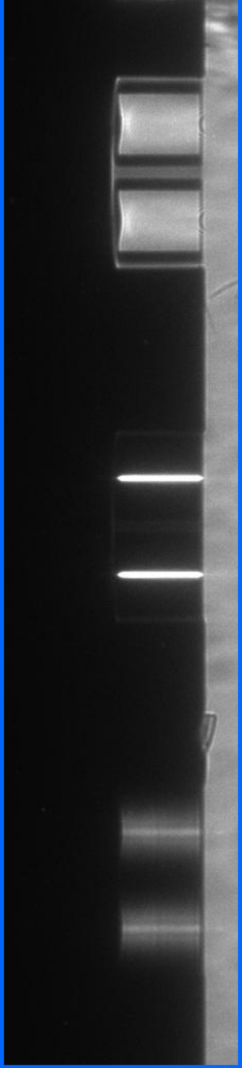

50 μm

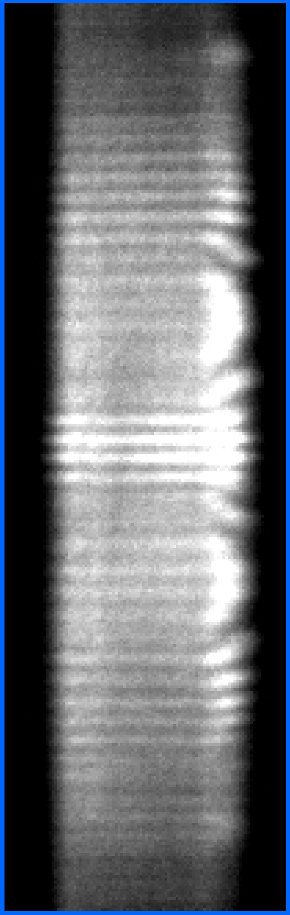

25 μm

E = 13 keV

Effective source size ~100 μm

Applications

- High energy X-ray microscopy: diffraction, spectroscopy, imaging
- Beam collimation for high resolution diffraction (< μrad)
- Beam shaping elements / Wave front correction
- Interferometry
- Beam diagnostics
- Optics for X-ray Free Electron Lasers

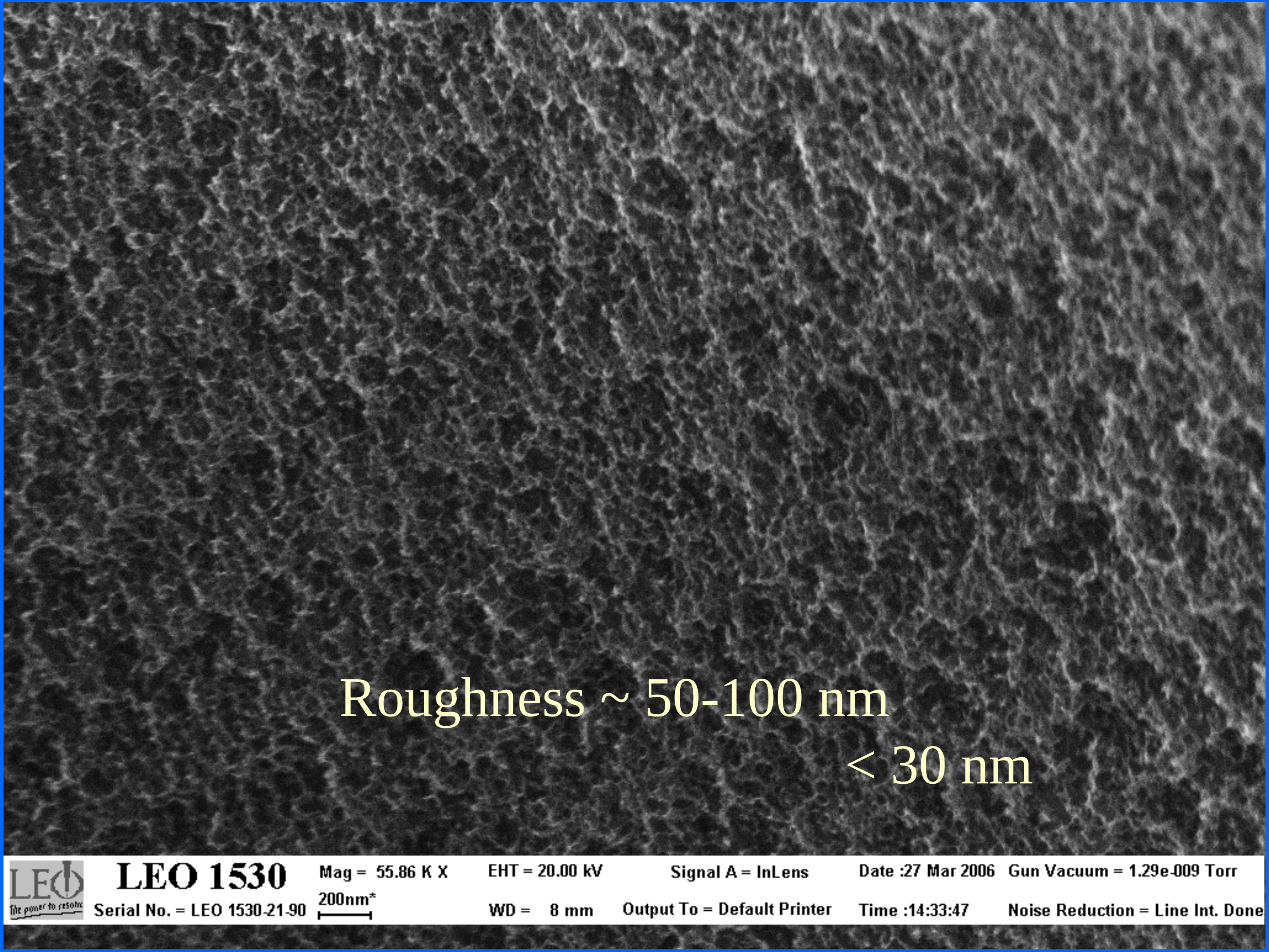

Roughness ~ 50-100 nm

< 30 nm

Integrated X-nanoprobe system

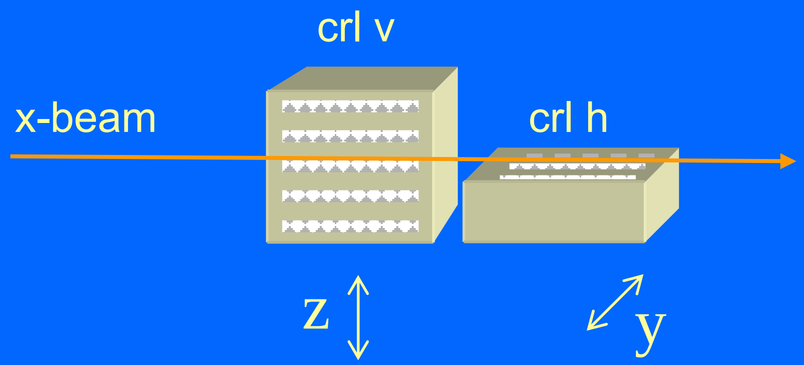

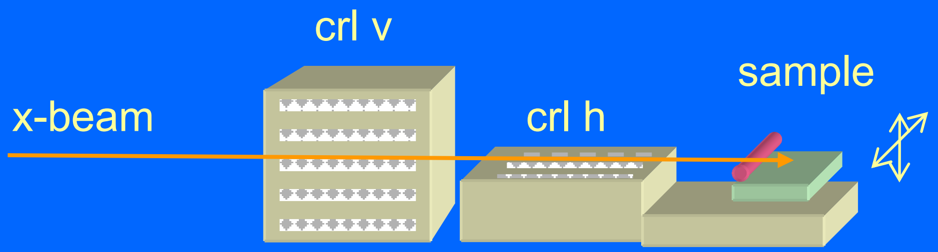

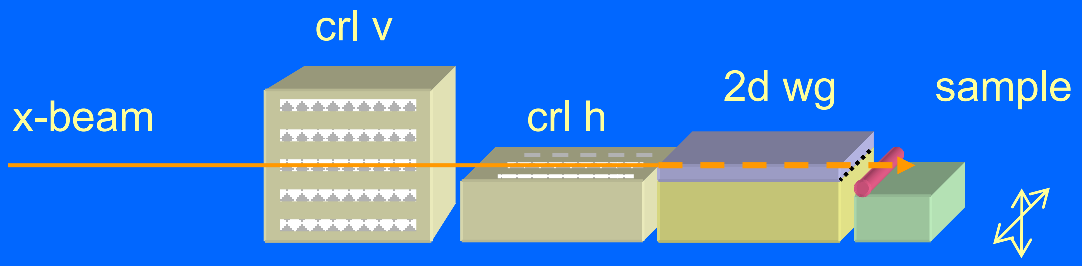

Planar parabolic lenses with scaled reduction of curvature radii

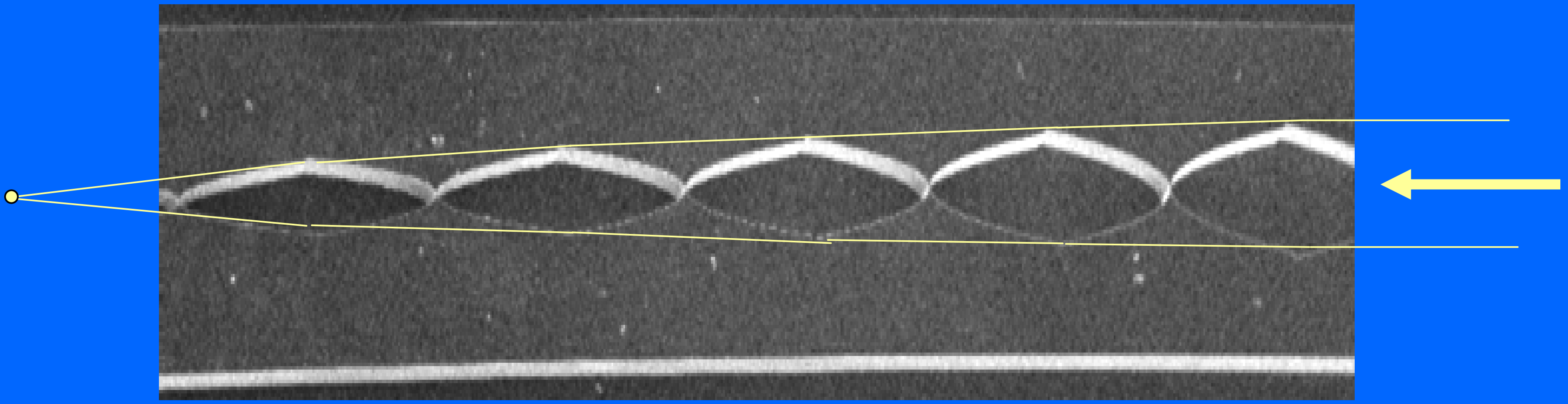

I. Snigireva, A. Snigirev, S. Kuznetsov, C. Rau, T. Weitkamp, L. Shabelnikov,
M. Grigoriev, V. Yunkin, M. Hoffmann, E. Voges,
"Refractive and diffractive optical elements", Proceedings of SPIE 4499, 64-74 (2001)

Number of lenses, *N*	Entrance radius	Aperture max.	Scaling factor, *q*	Exit radius
20	250 µm	500 µm	0.93	63 µm

E = 17.45 keV / F = 25 cm

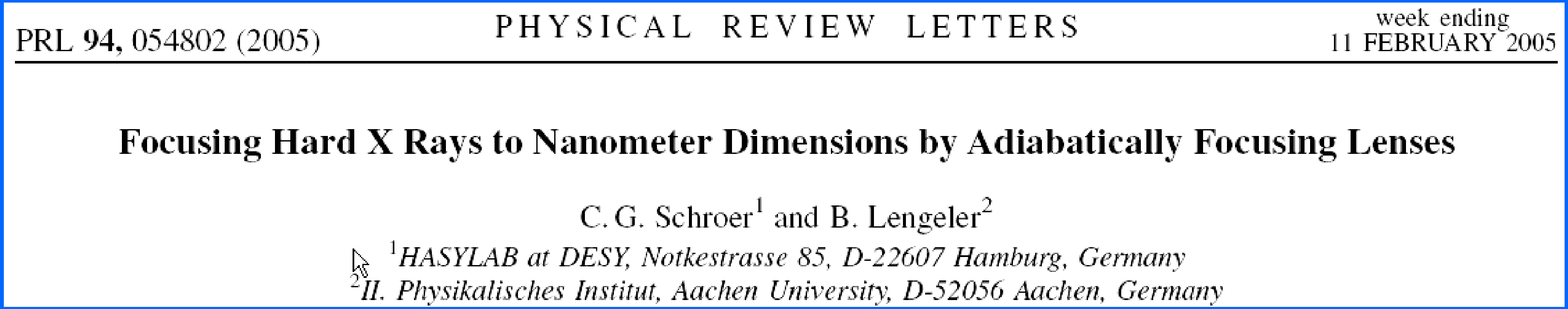

PRL **94,** 054802 (2005) PHYSICAL REVIEW LETTERS week ending 11 FEBRUARY 2005

Focusing Hard X Rays to Nanometer Dimensions by Adiabatically Focusing Lenses

C. G. Schroer[1] and B. Lengeler[2]
[1]*HASYLAB at DESY, Notkestrasse 85, D-22607 Hamburg, Germany*
[2]*II. Physikalisches Institut, Aachen University, D-52056 Aachen, Germany*

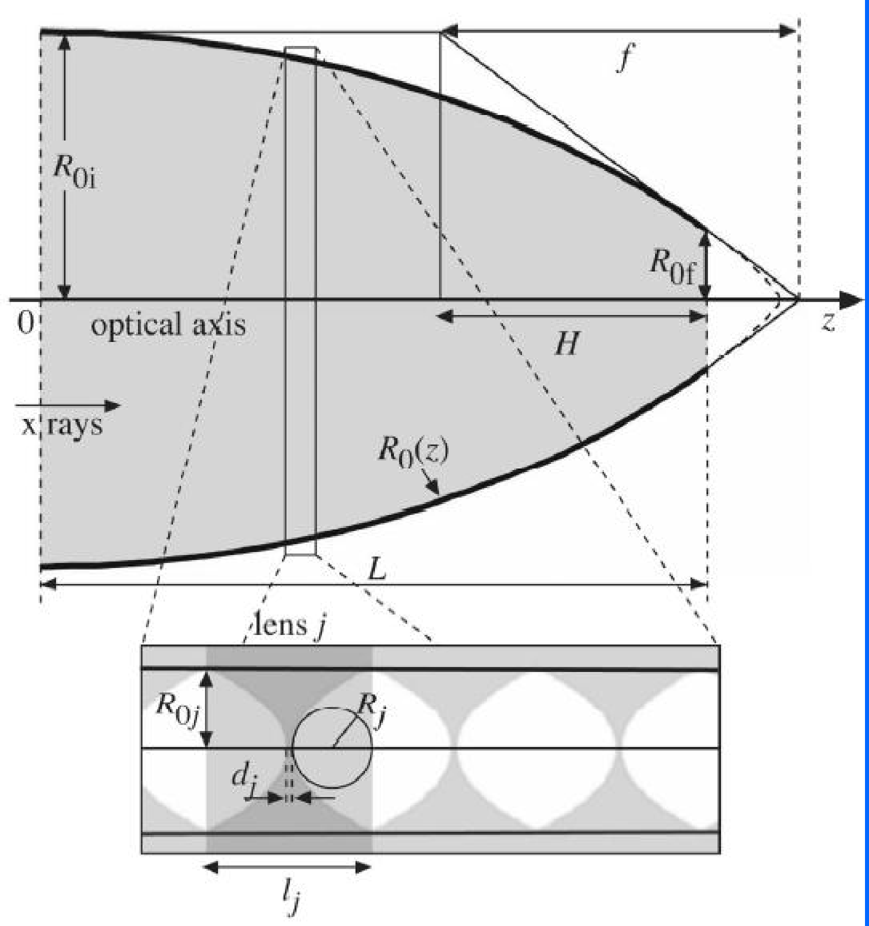

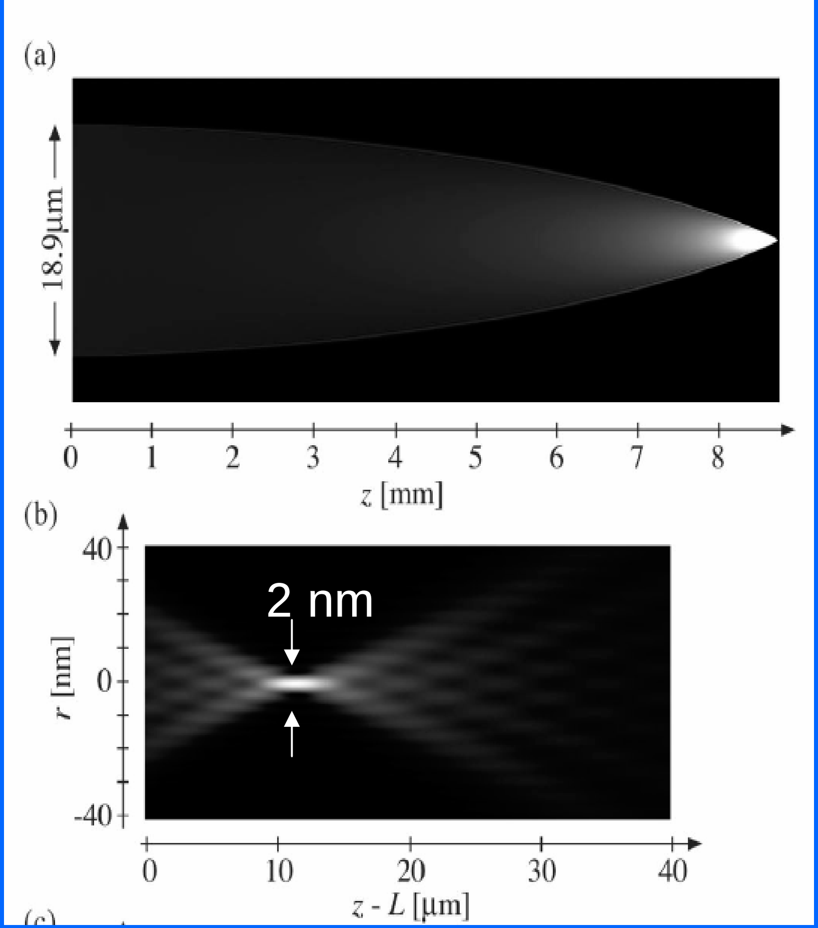

Si lens with minimized absorption

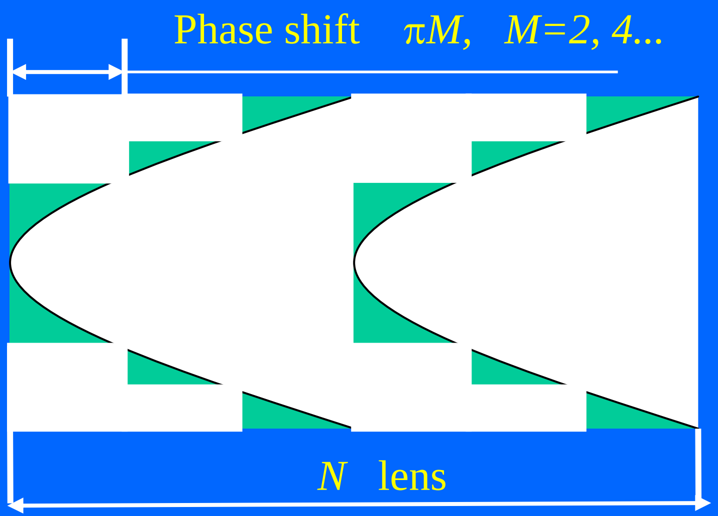

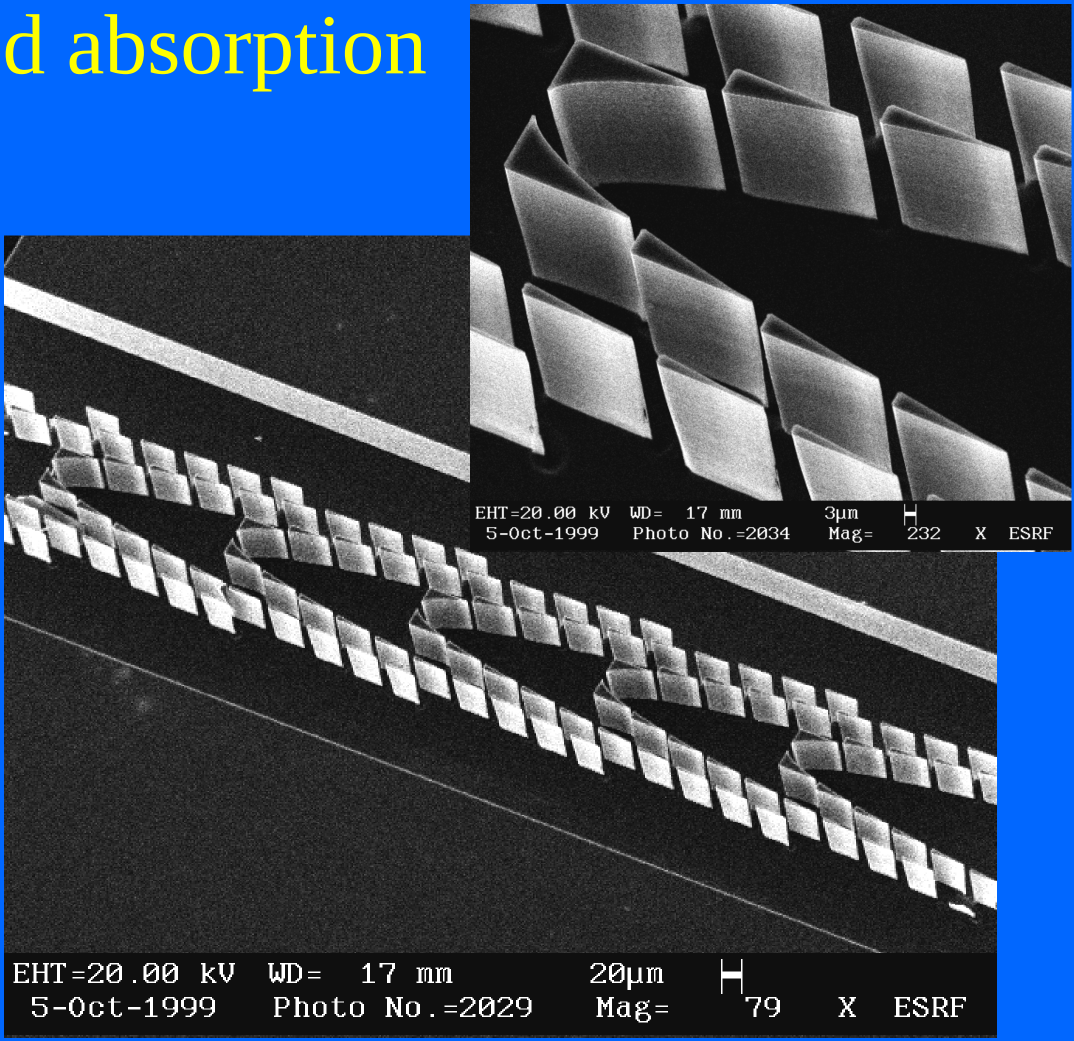

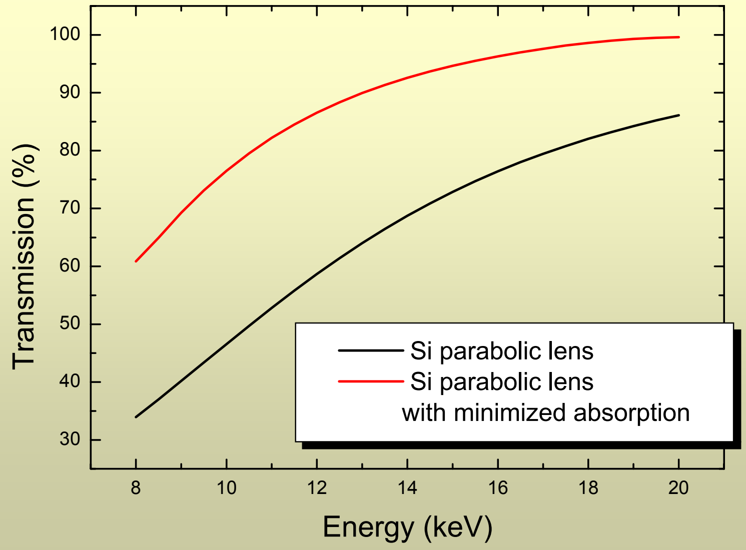

Aperture = 150 µm   Height = 100 µm

Number of lenses 5   N of segment pairs 10

$R_{\text{parabola apex}} = 12.72\ \mu m$

For   E = 17 keV   F = 80 cm

“Fern”- like profile Si lens

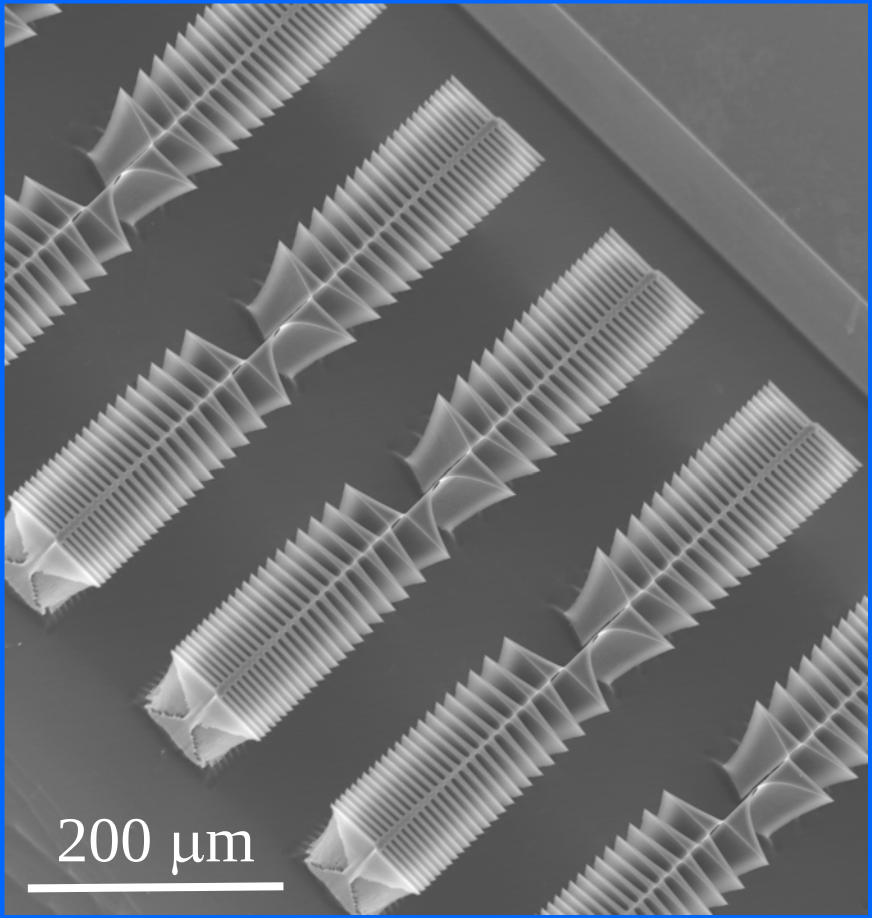

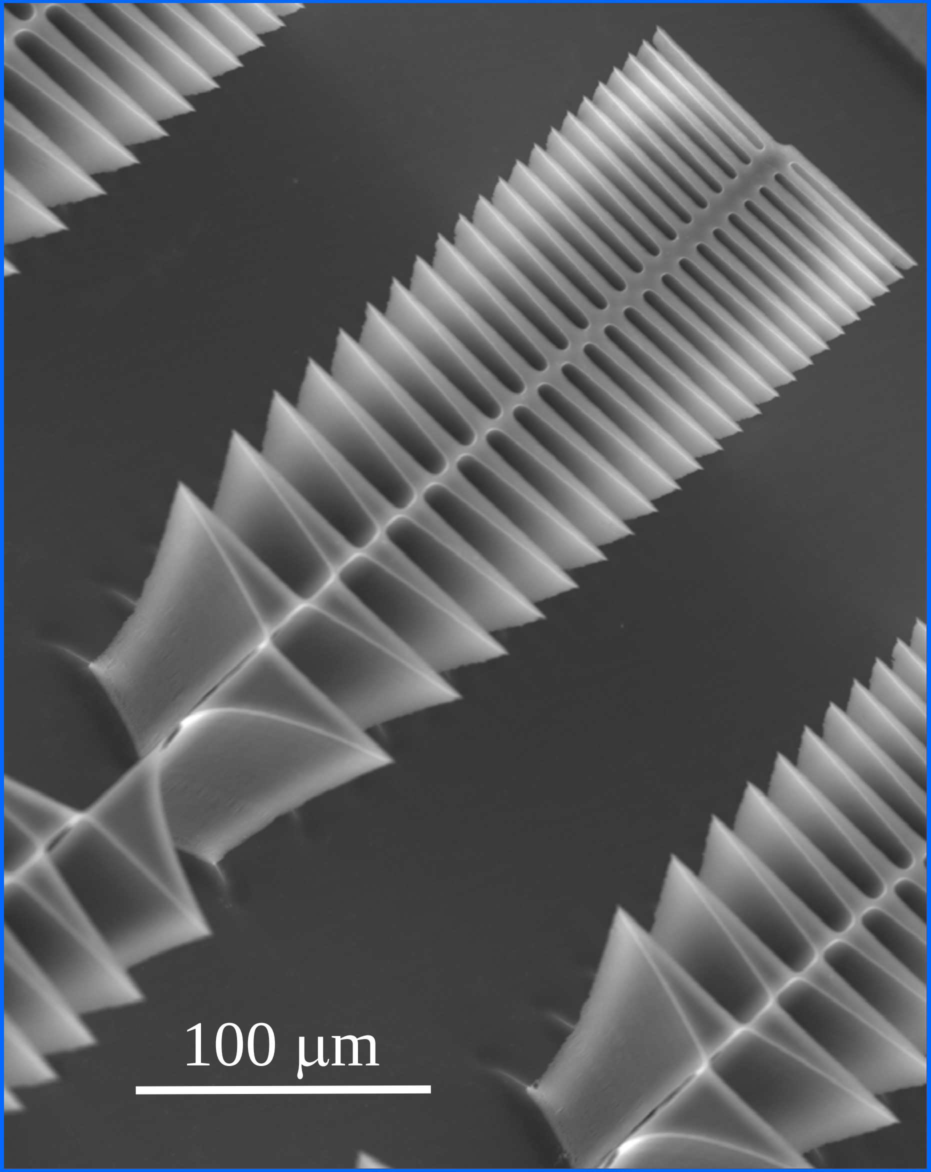

A = 505 μm
20 lenses
Δr_n=2.8 μm

E=17.48 keV
45 zones
2π phase shift

Refractive lens with kinoform profile (inline segments) has minimum total length but this dsign is complicated for realisation due to extremely wide range of feature width.
To narrow this range “fern”- like profile is proposed where even (or odd) segments are inverted

Richard M. Bionta

Prototype Focusing Element for the LCLS Warm Dense Matter Experiment

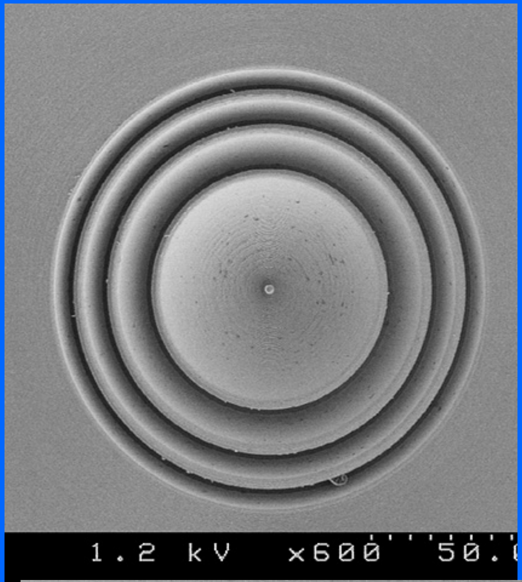

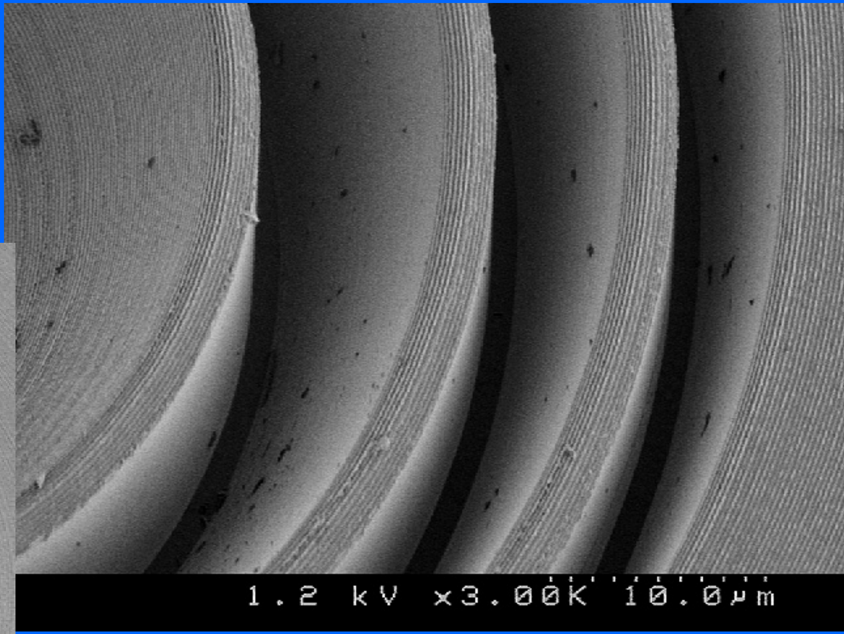

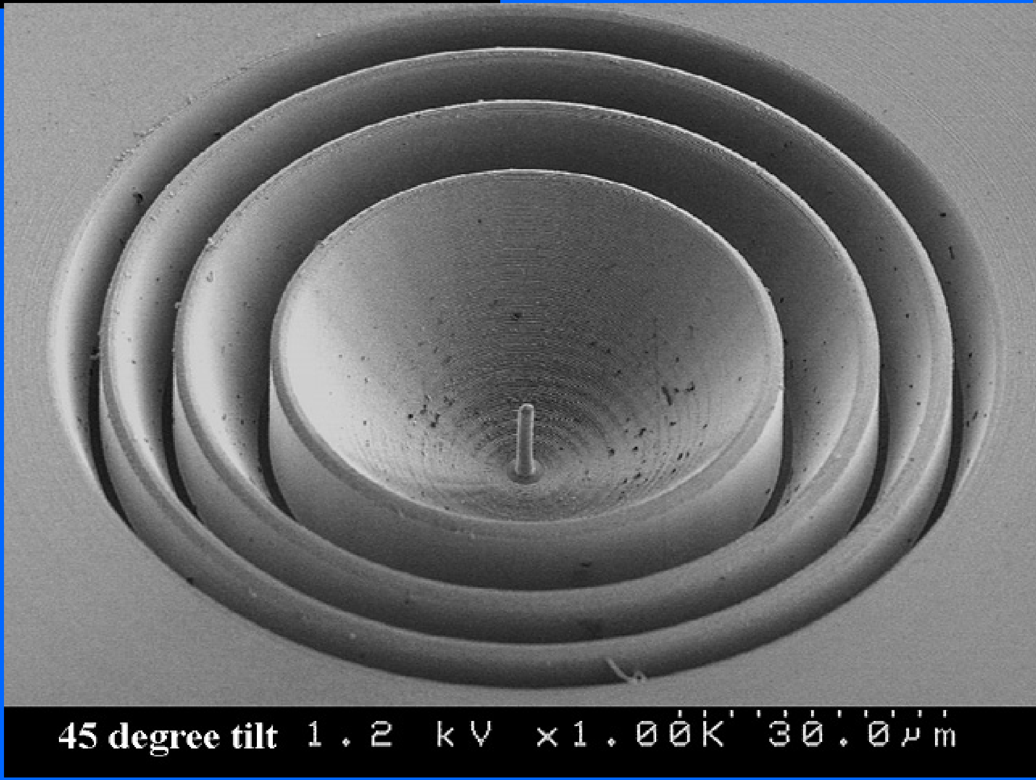

"blazed phase lens"
Diam. 100 µm
Al 79 µm
Groove hight 18.7 µm
Designed for 8 keV

Bragg-Fresnel Optics

<u>Bragg-Fresnel optics</u>
based on

- Crystal
- Multilayer
- Photonic crystals

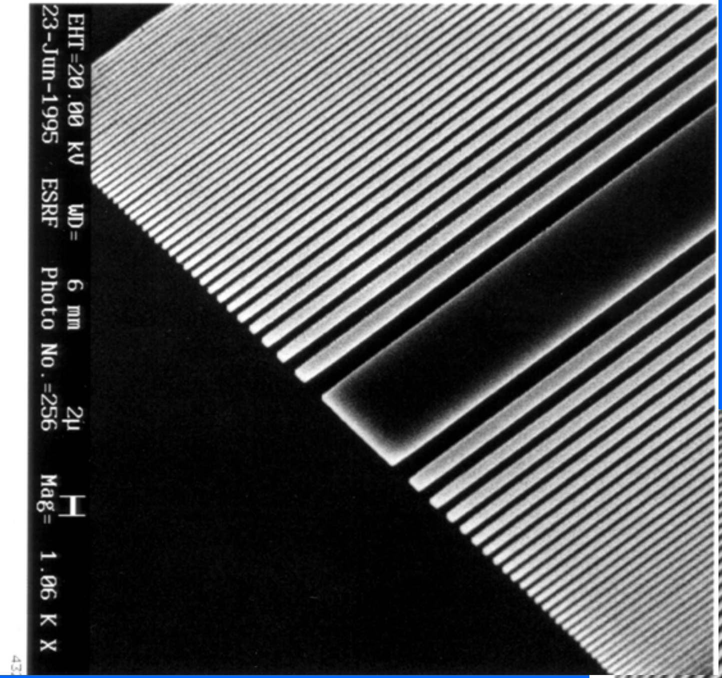

Linear BFL
Si (111)
A = 200 µm
Δr_n = 0.3 µm

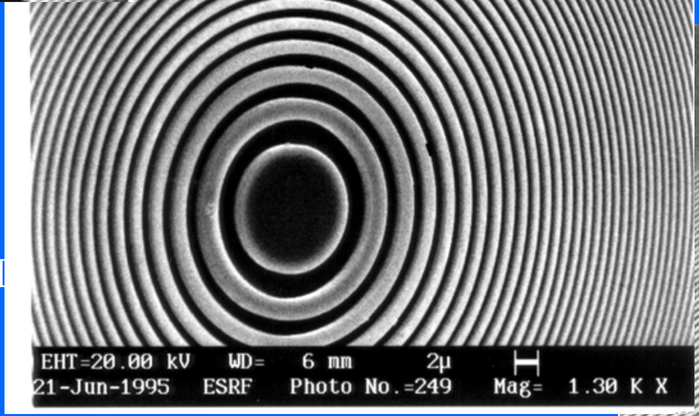

Circularar BFL
Ge (111)
A = 200 µm
Δr_n = 0.3 µm

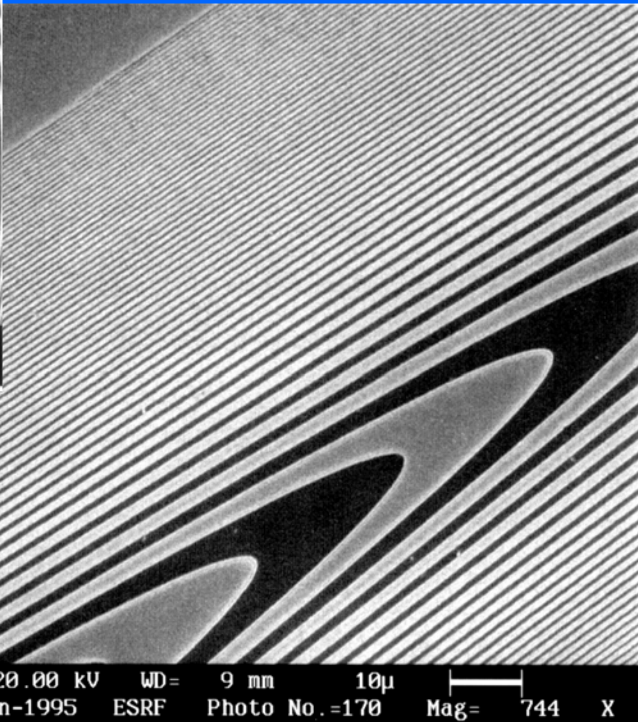

Multilayer BFL elliptical
W / Si, 56 periods
length = 18 mm
width = 136 µm
Δr_n = 0.3 µm

Microfluidics of soft matter investigated by small-angle X-ray scattering

Alexander Otten, Sarah Ko¨ster, Bernd Struth, Anatoly Snigirev and Thomas Pfohl

J. Synchrotron Rad. (2005). 12, 745–750

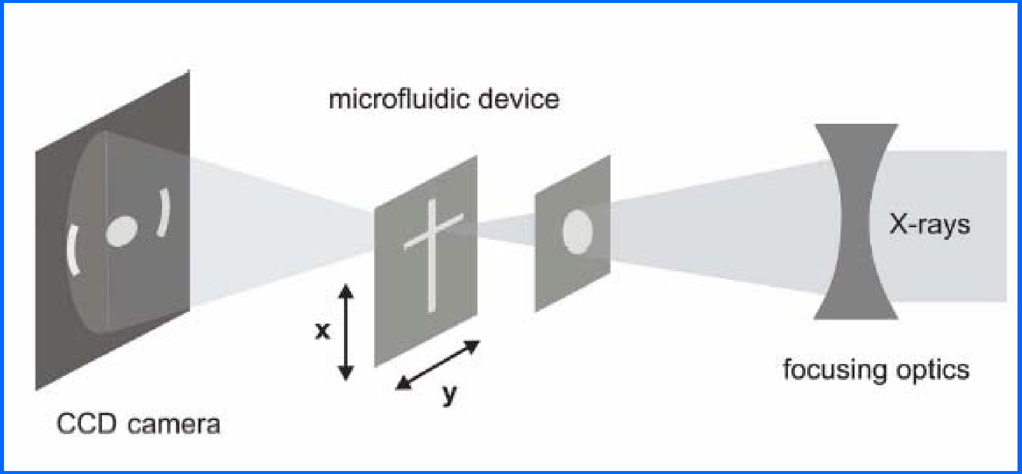

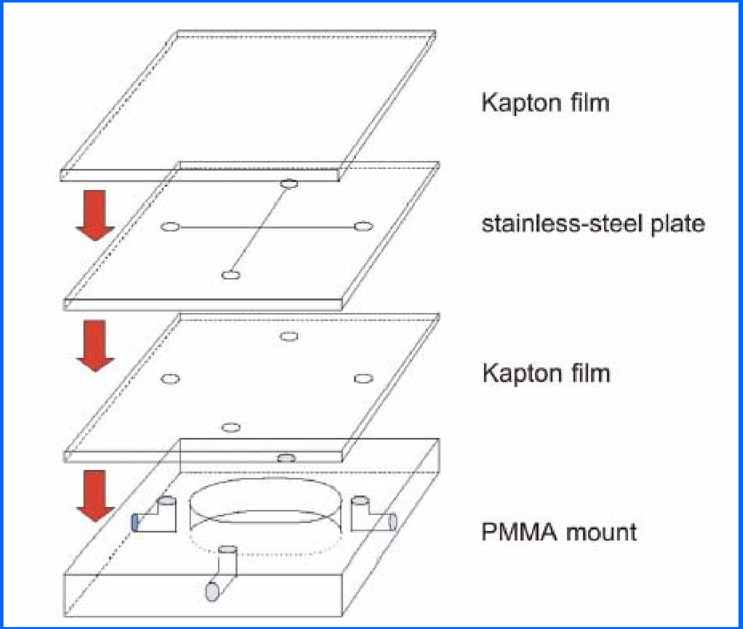

design of the microfluidic device

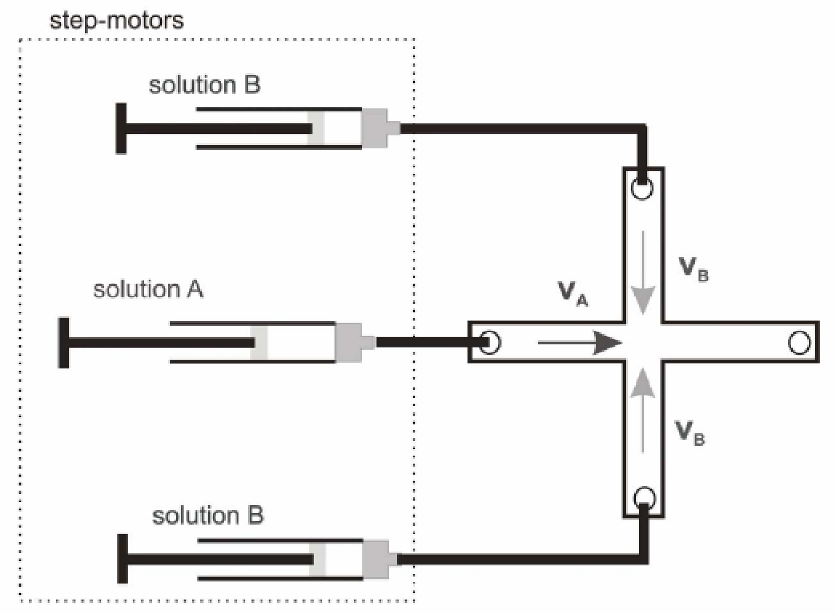

microfluidic pumping system.

Microfluidics: microbeam small-angle X-ray scattering

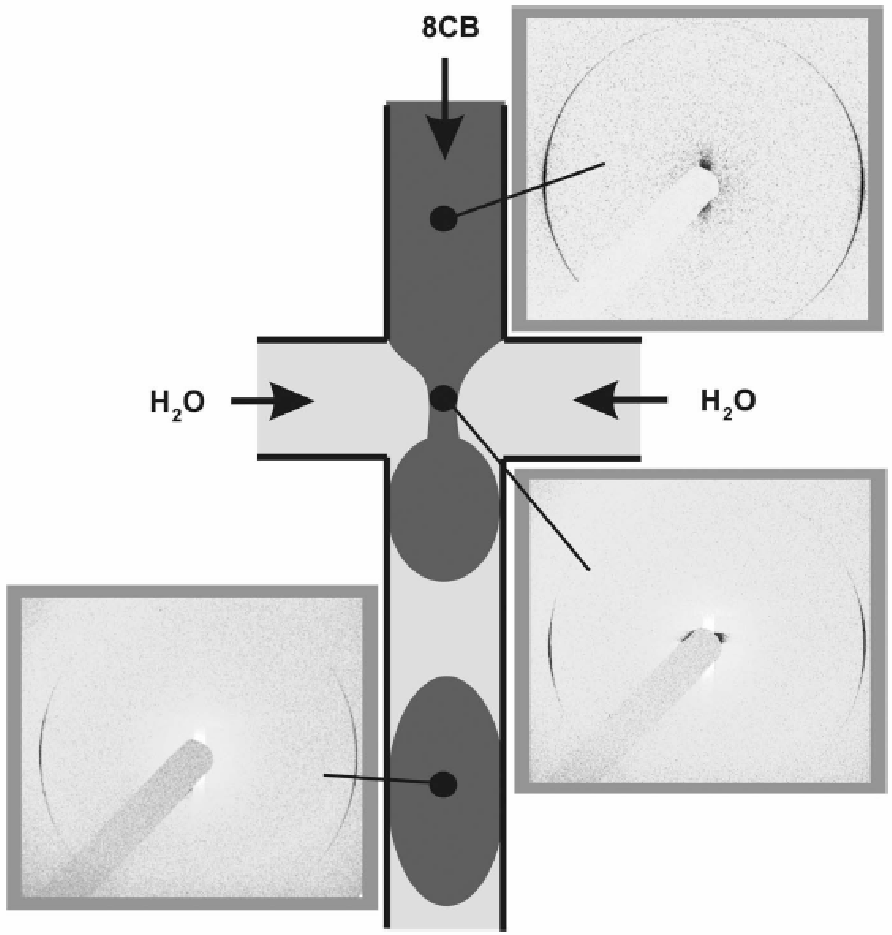

Schematic of the 8CB droplet formation with diffraction patterns observed at three different observation positions along the formation process.

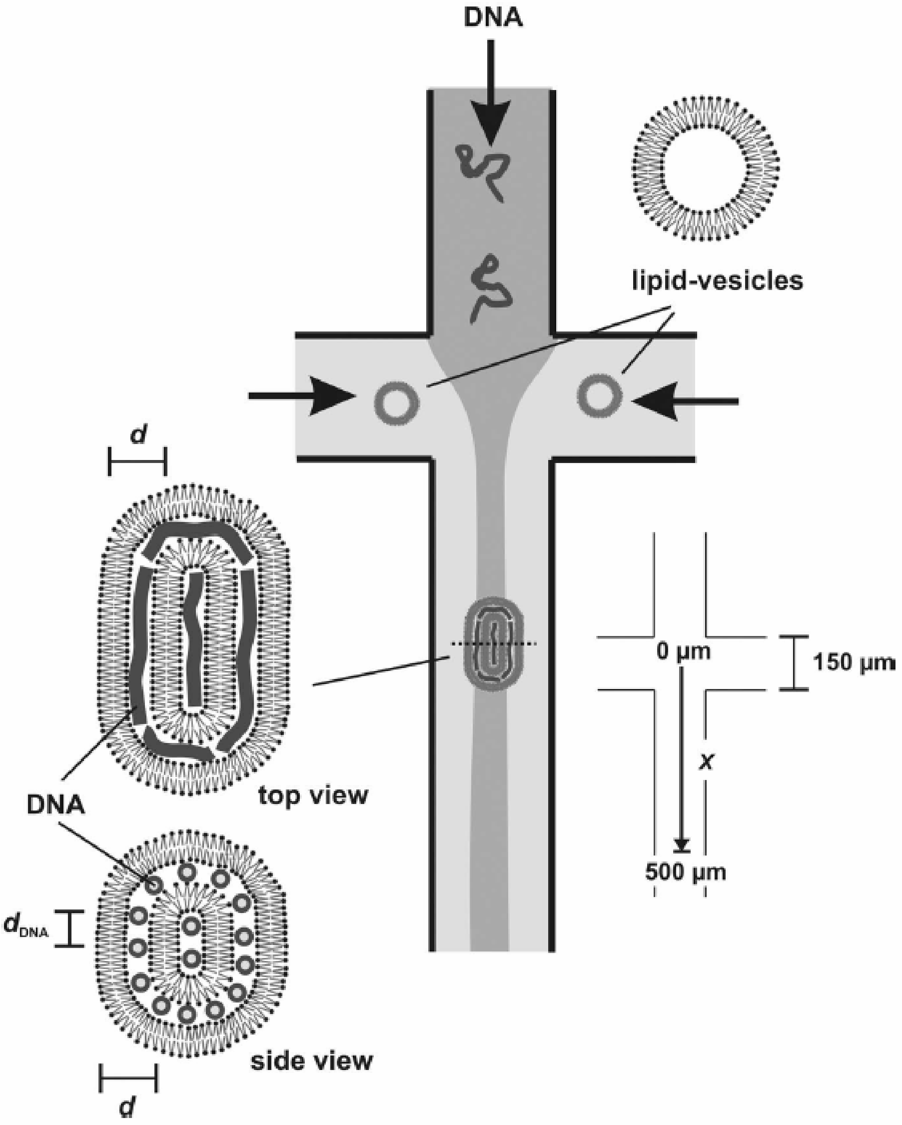

Schematic of the self-assembling of DNA multilamellar membranes in a hydrodynamic focusing and mixing device.

Alexander Otten, Sarah Köster, Bernd Struth,
Anatoly Snigirev and Thomas Pfohl.
J. Synchrotron Rad. (2005). 12, 745–750

Fourier Transform Diffraction/Imaging

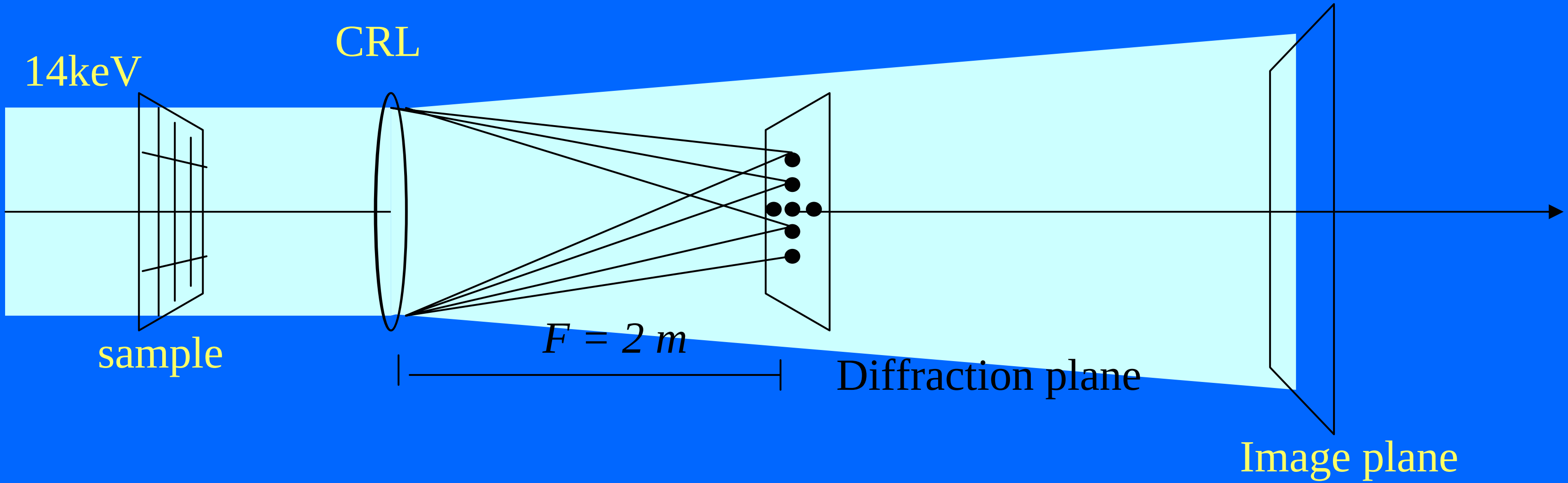

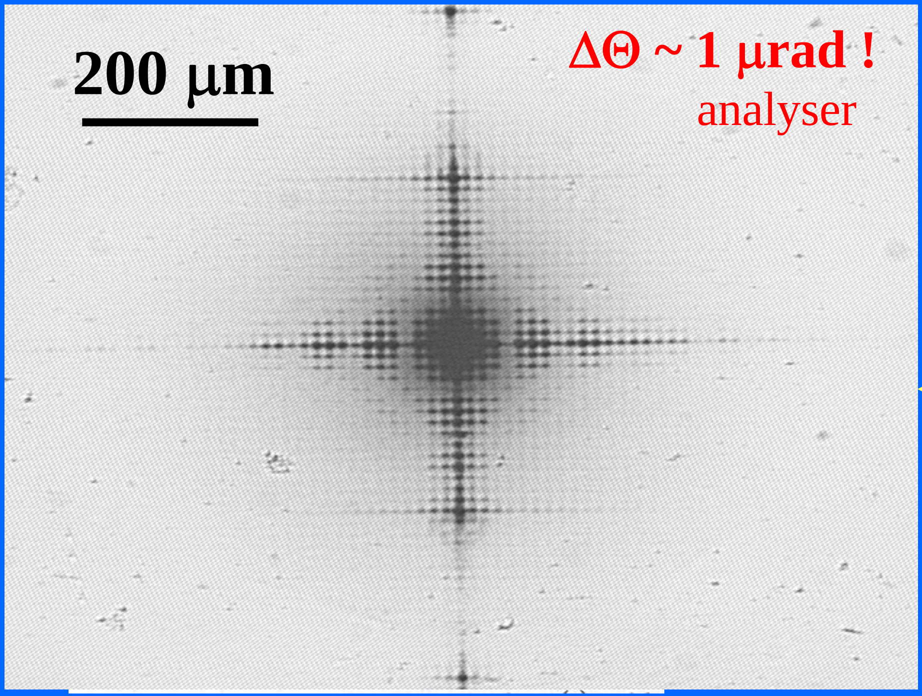

FT

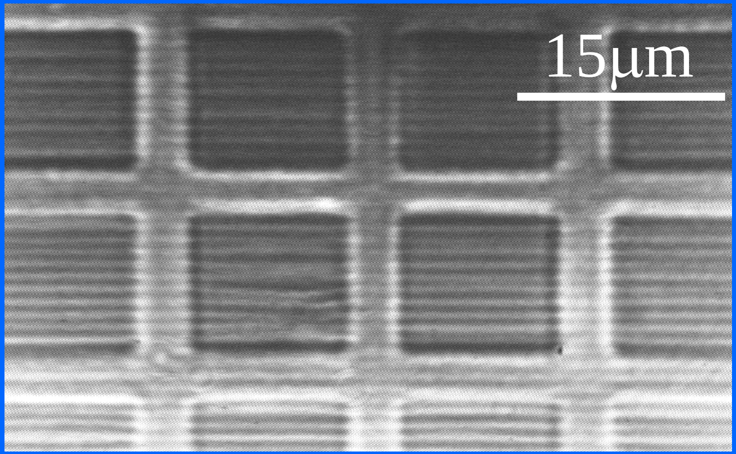

APPLIED PHYSICS LETTERS **86**, 014102 (2005)

X-ray high-resolution diffraction using refractive lenses

Michael Drakopoulos
Diamond Light Source Ltd., Chilton, Oxfordshire OX11 0QX, United Kingdom

Anatoly Snigirev and Irina Snigireva
European Synchrotron Radiation Facility, 38043 Grenoble, France

Jörg Schilling
California Institute of Technology, Pasadena, California 91125

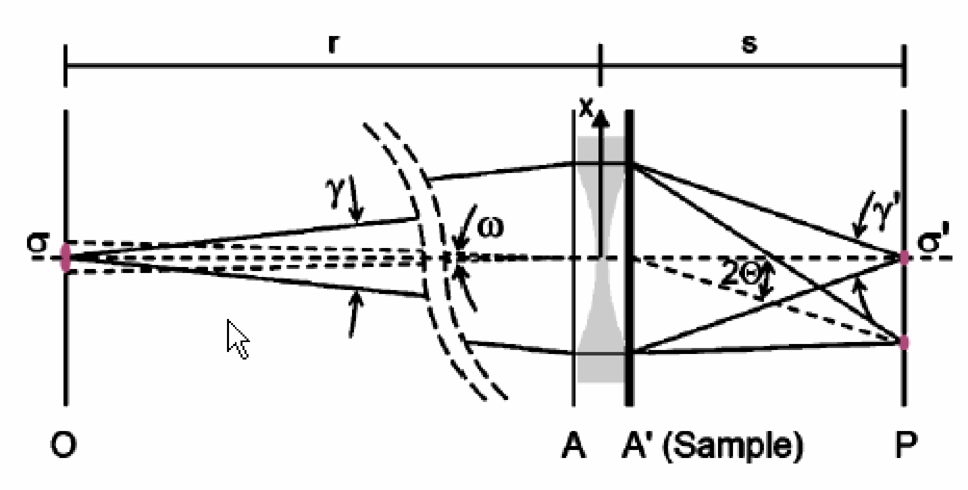

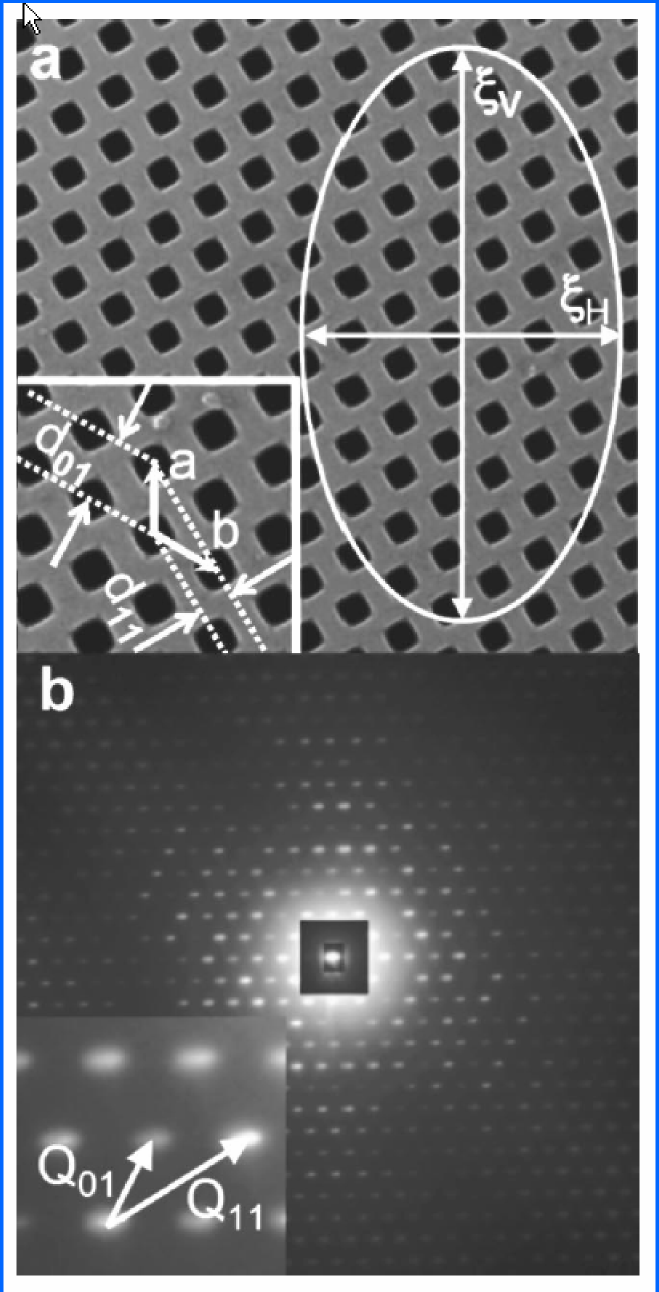

Theory: the Bragg law

Ordinary (atomic) crystals: $d \sim \lambda$
=> large diffraction angle 2θ

X-rays: $\lambda \sim 1$ A

$$\boxed{\sin\theta = n\lambda/2d; \quad n = 1, 2, \ldots}$$

Colloidal crystals: $d >> \lambda$
=> small diffraction angle 2θ
(10^{-4} … 10^{-3} radian)

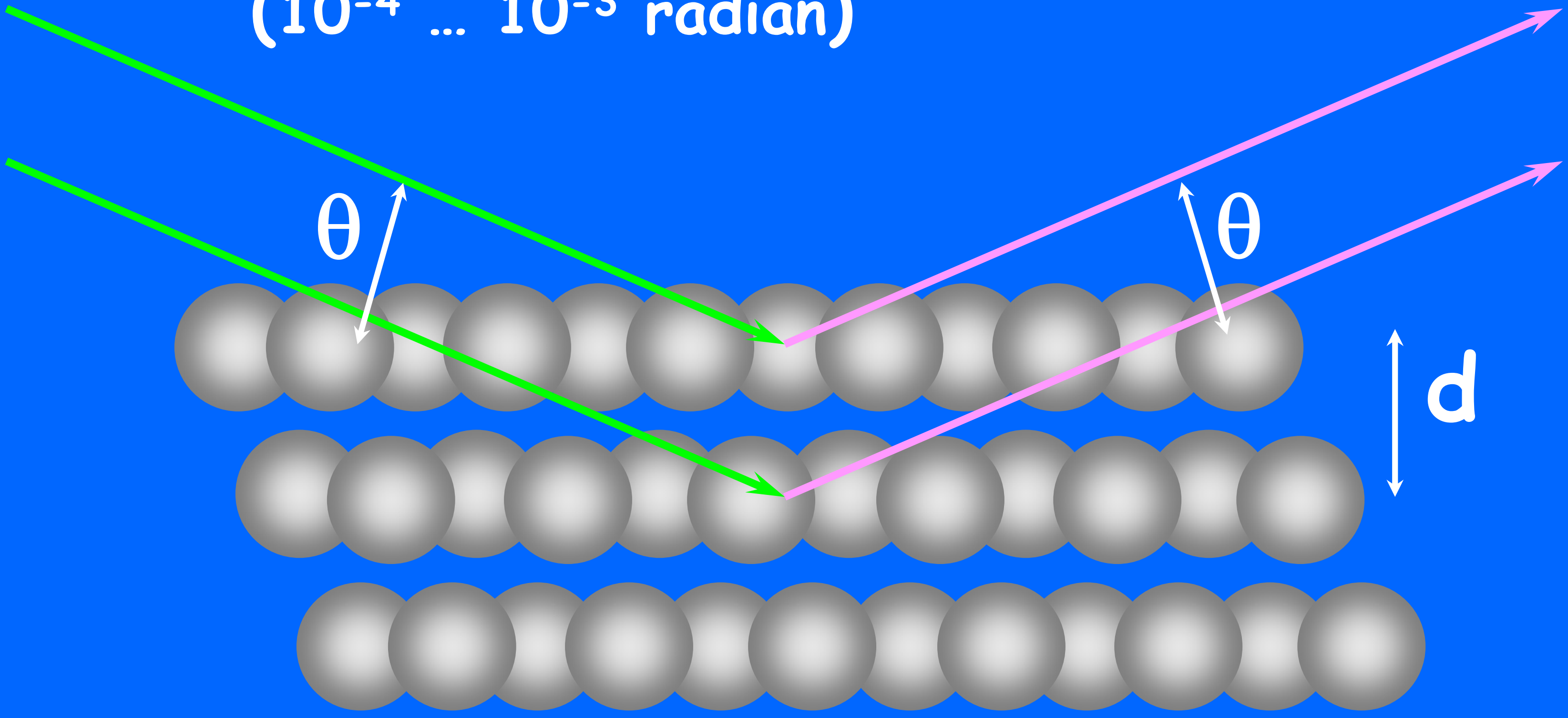

Latest news:

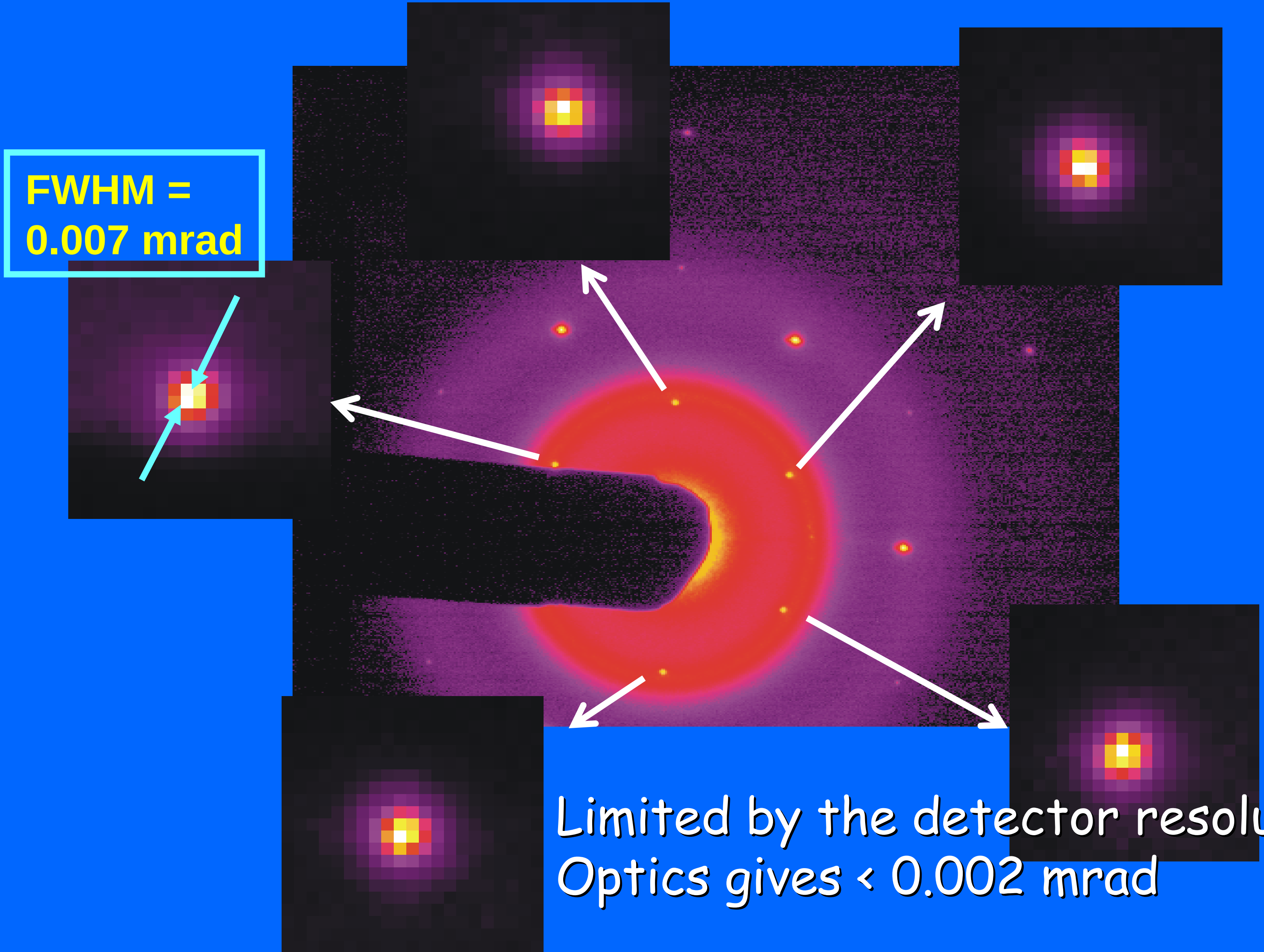
FWHM = 0.007 mrad

Limited by the detector resolution;
Optics gives < 0.002 mrad

Microelectronics / nanotechnology applications

SOI technology – strained Si - charge carrier mobility

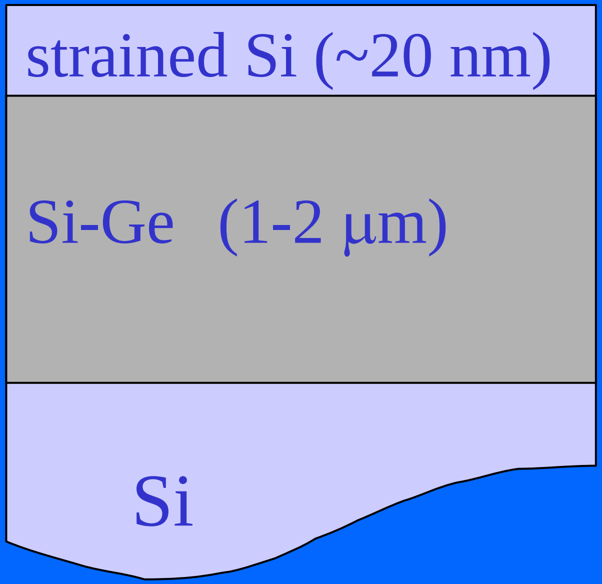

Needs:
- Local strain analysis
- Depth structure analysis of dislocations
    - resolutionn < 10 nm !

    wafer level ➡ transistor level

TEM: converging e-beam diffraction

    problems:
    - does not see dislocation density <10^4
    - sample preparation
        thin sample – relaxations!

X –ray diffraction microscopy

    converging coherent x-ray beam diffraction ?

The first experiments with ERL will very quickly develop new classes of experiments as they gain experience with their unique source properties